

Electronic Supplementary Material for

Difuryl(supermesityl)borane: a versatile building block for extended π -conjugated materials

Nicolas A. Riensch,[§] Lars Fritze,[§] Tobias Schindler, Marius Kremer and Holger Helten*

Institute of Inorganic Chemistry, RWTH Aachen University, Landoltweg 1, 52056 Aachen, Germany

Email: holger.helten@ac.rwth-aachen.de

§ These authors contributed equally to this work.

Content

1 Experimental Section

General procedures

Syntheses

X-ray crystallography

NMR spectra

UV–vis spectra

Fluorescence spectra

Mass spectra

Cyclic Voltammetry

2 Computational Information

References

1 Experimental Section

General procedures. All manipulations were performed under an atmosphere of dry argon using standard Schlenk techniques or in an MBraun glove box. Solvents (dichloromethane, *n*-pentane, diethylether, toluene, and tetrahydrofuran) were dried and degassed by means of an MBraun SPS-800 solvent purification system. *N,N'*-Dimethylformamide was dried over MgSO₄ and distilled prior to use. Deuterated solvents for NMR spectroscopy were dried and degassed at reflux over Na (C₆D₆) or CaH₂ (CDCl₃ and CD₂Cl₂) and freshly distilled prior to use. *n*-Hexane for aqueous work-up, tribromoborane, bromobenzene, thiophene, magnesium turnings, iodine, bromine, and Pd(PPh₃)₄ were purchased from commercial sources and used as received. Solutions of *n*-butyllithium (1.6 M and 2.5 M in hexane, respectively) and *tert*-butyllithium (1.7 M in pentane) were purchased from Sigma Aldrich and used as received as well. Furan and 2-isopropoxy-4,4,5,5-tetramethyl-1,3,2-dioxaborolane were commercially purchased and freshly distilled prior to use. Compound **1**,^[1a] 4,4,5,5-tetramethyl-2-(2-thienyl)-1,3,2-dioxaborolane,^[1b] and 4,4,5,5-tetramethyl-2-(2-furyl)-1,3,2-dioxaborolane^[1c] were prepared according to methods described in the literature. NMR spectra were recorded at 25 °C on a Bruker Avance II-400 spectrometer or on a Bruker Avance III HD spectrometer operating at 400 MHz. Chemical shifts were referenced to residual protic impurities in the solvent (¹H) or the deuterio solvent itself (¹³C) and reported relative to external SiMe₄ (¹H, ¹³C) or BF₃·OEt₂ (¹¹B) standards. Mass spectra were obtained with the use of a Finnigan MAT95 spectrometer employing electron ionization (EI) using a 70 eV electron impact ionization source. Elemental analysis was performed with a CHN-O-Rapid VarioEL by Heraeus. UV–vis spectra were obtained using a Jasco V-630 spectrophotometer. Fluorescence spectra were obtained with a Jasco FP-6600 spectrofluorometer. Fluorescence quantum yields were determined against perylene as the standard. Melting points (uncorrected) were obtained using a SMP3 melting point apparatus by Stuart in 0.5 mm (o.d.) glass capillaries. Cyclic voltammetry (CV) experiments were carried out on a PGSTAT101 analyzer from Metrohm. The three-electrode system consisted of a Pt disk as working electrode, a Pt wire as counter electrode, and an Ag wire as the reference electrode. The voltammograms were recorded with ca. 10⁻³ M solutions in THF containing Bu₄N[PF₆] (0.1 M) as the supporting electrolyte. The scans were referenced after the addition of a small amount of ferrocene as internal standard. The potentials are reported relative to the ferrocene/ferrocenium couple.

Synthesis of 2a. To a solution of **1** (468.4 mg, 1.20 mmol) in Et₂O (9.0 mL) was added *tert*-butyllithium (1.7 M, 1.45 mL, 2.46 mmol) at -78 °C. Subsequently, the mixture was warmed to room temperature and stirred for further 3 h. Then, bromine (479.4 mg, 3.00 mmol) was added at -78 °C. The reaction mixture was allowed to warm up to room temperature overnight. All volatiles were removed *in vacuo*, and the brownish crude product was subjected to column

chromatography (AlOx; *n*-hexane) to give **2a** as a colorless solid (m.p. 179.4 °C). Yield: 505.7 mg (0.92 mmol, 77 %); ¹H NMR (400 MHz, CDCl₃): δ = 7.42 (s, 2H, Mes^{*}-CH), 7.30–6.95 (br, 2H, Fur-H), 6.44 (d, ³J_{HH} = 3.4 Hz, 2H, Fur-H), 1.39 (s, 9H, *p*-^tBu-CH₃), 1.19 (s, 18H, *o*-^tBu-CH₃); ¹¹B{¹H} NMR (128 MHz, CDCl₃): δ = 46.1 (s); ¹³C{¹H} NMR (101 MHz, CDCl₃): δ = 166.8 (Fur-C-B), 152.7 (Mes^{*}-C-*o*-^tBu), 148.9 (Mes^{*}-C-*p*-^tBu), 130.7 (Mes^{*}-C-B, Fur-CH), 129.7 (Fur-CBr), 122.1 (Mes^{*}-CH), 113.7 (Fur-CH), 38.4 (*o*-^tBu-C), 34.9 (*p*-^tBu-C), 34.4 (*o*-^tBu-CH₃), 31.6 (*p*-^tBu-CH₃); MS (EI, 70 eV): *m/z* (%) = 548.1 ([M]⁺, 45), 231.2 (C₆H₂-ⁱPr-(^tBu)₂)⁺, 72), 151.1 ([C₁₀H₄BO]⁺, 51), 77.1 ([Ph]⁺, 100); elem. anal. calcd (%) for C₂₆H₃₃BBr₂O₂: C 56.97, H 6.07, found: C 57.26, H 6.08; UV-vis (THF): λ_{abs,max} = 332 nm (ε = 26967 L mol⁻¹ cm⁻¹); fluorescence (THF): non-emissive.

Synthesis of 2b. To a solution of **1** (780.7 mg, 2.00 mmol) in Et₂O (15 mL) was added *tert*-butyllithium (1.7 M, 2.41 mL, 4.10 mmol) at -78 °C. Subsequently, the mixture was warmed to room temperature and stirred for further 3 h. Then, a solution of iodine (1.27 g, 5.00 mmol) in THF (2.5 mL) was added at -78 °C. The reaction mixture was allowed to warm up to room temperature overnight. All volatiles were removed *in vacuo*, and the brownish crude product was subjected to column chromatography (silica; *n*-hexane) and sublimation to remove residual iodine to give **2b** as a colorless solid (m.p. 204.5 °C). Yield: 1.03 g (1.60 mmol, 80 %); ¹H NMR (400 MHz, CDCl₃): δ = 7.41 (s, 2H, Mes^{*}-CH), 7.20–6.90 (br, 2H, Fur-H), 6.66 (d, ³J_{HH} = 3.4 Hz, 2H, Fur-H), 1.38 (s, 9H, *p*-^tBu-CH₃), 1.17 (s, 18H, *o*-^tBu-CH₃); ¹¹B{¹H} NMR (128 MHz, CDCl₃): δ = 45.9 (s); ¹³C{¹H} NMR (101 MHz, CDCl₃): δ = 170.5 (Fur-C-B), 152.7 (Mes^{*}-C-*o*-^tBu), 148.8 (Mes^{*}-C-*p*-^tBu), 130.8 (Mes^{*}-C-B, Fur-CH), 122.3 (Fur-CH), 122.0 (Mes^{*}-CH), 97.4 (Fur-CH), 38.4 (*o*-^tBu-C), 34.9 (*p*-^tBu-C), 34.4 (*o*-^tBu-CH₃), 31.6 (*p*-^tBu-CH₃); MS (EI, 70 eV): *m/z* (%) = 642.1 ([M]⁺, 4), 246.3 ([BH₂Mes^{*}]⁺, 69), 232.4 ([C₆H₃-ⁱPr-(^tBu)₂)⁺, 100); elem. anal. calcd (%) for C₂₆H₃₃BI₂O₂: C 48.63, H 5.18, found: C 49.89, H 5.25; UV-vis (THF): λ_{abs,max} = 341 nm (ε = 31466 L mol⁻¹ cm⁻¹); fluorescence (THF): non-emissive.

Synthesis of 3. Compound **2a** (109.6 mg, 0.20 mmol) and 4,4,5,5-tetramethyl-2-(2-thienyl)-1,3,2-dioxaborolane (85.1 mg, 0.405 mmol) were charged into a Schlenk flask. Subsequently, dry DMF (3 mL) and toluene (3 mL) were added and the mixture was degassed by freeze-pump-thaw cycles. Then, Pd(PPh₃)₄ (15 mol%) followed by K₂CO₃ (164.4 mg, 1.190 mmol) were added under nitrogen. The reaction mixture was heated at 120 °C for 18 hours with vigorous stirring. Then, the mixture was cooled to ambient temperature and diluted with DCM (10 mL). After filtration, all volatiles were removed *in vacuo*, and the product was purified by column chromatography with gradient (hexane:DCM 100:0 → 80:20). Compound **3** was obtained as a yellow solid (m.p. 184.9 °C). Yield: 62 mg (0.11 mmol, 56 %); ¹H NMR (400 MHz, CDCl₃): δ = 7.37 (s, 2H, Mes^{*}-CH), 7.34 (br d, ³J_{HH} = 2.8 Hz, 2H, Thi-H), 7.20 (d, ³J_{HH} = 5.0 Hz, 2H, Thi-H), 6.96–6.94 (dd, ³J_{HH} = 3.5 Hz, ⁴J_{HH} = 1.8 Hz, 2H, Thi-H), 6.54 (d, ³J_{HH} = 3.0 Hz, 2H,

Fur-*H*), 1.34 (s, 9H, *p*-Mes^{*}-CH₃), 1.17 (s, 18H, *o*-Mes^{*}-CH₃); ¹¹B{¹H} NMR (128 MHz, CDCl₃): δ = 47.2 (s); ¹³C{¹H} NMR (101 MHz, CDCl₃): δ = 163.7 (Fur-C-B), 154.3 (Fur-C-C_{Thi}), 152.3 (Mes^{*}-C-*o*-^tBu), 148.1 (Mes^{*}-C-*p*-^tBu), 133.7 (Thi-C-C_{Fur}), 132.2 (Mes^{*}-C-B), 130.1 (Fur-CH), 127.7 (Thi-CH), 125.3 (Thi-CH), 124.0 (Thi-C), 121.5 (Mes^{*}-CH), 107.0 (Fur-C), 38.3 (*o*-^tBu-C), 34.3 (*p*-^tBu-C), 31.5 (*o*-^tBu-CH₃), 31.3 (*p*-^tBu-CH₃); MS (EI, 70 eV): *m/z* (%) = 553.7 ([M]⁺, 3), 471.7 ([Mes^{*}BFur₂Thi]⁺, 3), 256.9 ([Mes^{*}B]⁺, 70), 230.9 (C₆H₂-^tPr-(^tBu)₂)⁺, 100); UV-vis (THF): λ_{abs,max} = 329 nm (ε = 60467 L mol⁻¹ cm⁻¹), 400 nm (ε = 115763 L mol⁻¹ cm⁻¹); fluorescence (THF): λ_{em,max} (λ_{ex}=400 nm) = 433 nm (Φ_f = 87.2 %); CV (THF): E_{1/2} = -2.48 V.

Synthesis of 4. Compound **2b** (128.4 mg, 0.20 mmol) and 4,4,5,5-tetramethyl-2-(2-furyl)-1,3,2-dioxaborolane (78.6 mg, 0.405 mmol) were charged into a Schlenk flask. Subsequently, dry DMF (3 mL) and toluene (3 ml) were added and the mixture was degassed by freeze-pump-thaw cycles. Then, Pd(PPh₃)₄ (15 mol%) followed by K₂CO₃ (164.4 mg, 1.190 mmol) were added under nitrogen. The reaction mixture was heated at 120 °C for 18 hours with vigorous stirring. Then, the mixture was cooled to ambient temperature and diluted with DCM (10 mL). After filtration, all volatiles were removed *in vacuo*, and the product was purified by column chromatography with gradient (hexane:DCM 100:0 -> 80:20). Compound **4** was obtained as a brownish solid (m.p. 125 °C). Yield: 34 mg (0.065 mmol, 33 %); ¹H NMR (400 MHz, CDCl₃): δ = 7.47 (d, ³J_{HH} = 1.7 Hz, 2H, Fur-*H*), 7.43 (s, 2H, Mes^{*}-CH), 7.39–7.06 (br, 2H, Fur-*H*), 6.74 (d, ³J_{HH} = 3.4 Hz, 2H, Fur-*H*), 6.70 (d, ³J_{HH} = 3.5 Hz, 2H, Fur-*H*), 6.50 (dd, ³J_{HH} = 3.5, ⁴J_{HH} = 1.8 Hz, 2H, Fur-*H*), 1.40 (s, 9H, *p*-Mes^{*}-CH₃), 1.22 (s, 18H, *o*-Mes^{*}-CH₃); ¹¹B{¹H} NMR (128 MHz, CDCl₃): δ = 46.9 (s); ¹³C{¹H} NMR (101 MHz, CDCl₃): δ = 164.3 (Fur-C-B), 152.9 (Mes^{*}-C-*o*-^tBu), 151.7 (Fur-C-C_{Fur}), 148.8 (Mes^{*}-C-*p*-^tBu), 147.2 (Fur-C-C_{Fur}), 143.1 (Fur-CH), 132.8 (Mes^{*}-C-B), 130.4 (Fur-CH), 122.1 (Mes^{*}-CH), 112.2 (Fur-CH), 107.7 (Fur-CH), 107.6 (Fur-CH), 38.8 (*o*-^tBu-C), 35.2 (*p*-^tBu-C), 34.8 (*o*-^tBu-CH₃), 31.9 (*p*-^tBu-CH₃); MS (EI, 70 eV): *m/z* (%) = 521.7 ([M]⁺, 37), 481.1 ([Ph-*p*-CH₃-*o*-(^tBu)₂)⁺, 63), 230.9 ([C₆H₂-^tPr-(^tBu)₂)⁺, 100); UV-vis (THF): λ_{abs,max} = 336 nm (ε = 45808 L mol⁻¹ cm⁻¹), 394 nm (ε = 107771 L mol⁻¹ cm⁻¹); fluorescence (THF): λ_{em,max} (λ_{ex}= 394 nm) = 427 nm (Φ_f = 67.0 %); CV (THF): E_{1/2} = -2.53 V.

X-ray crystallographic analysis

Suitable single crystals of **2a** (CCDC 1840367) and **2b** (CCDC 1840368) were obtained by slow evaporation of dichloromethane at 4 °C. **3** (CCDC 1843527) was obtained by slow evaporation of hexane at -40 °C. Data were collected on a Bruker SMART APEX CCD detector on a D8 goniometer equipped with an Oxford Cryostream 700 temperature controller at 100(2) K using graphite monochromated Mo-*K*_α radiation (λ = 0.71073 Å). An absorption correction was carried out semi-empirically using SADABS^[2]. The structures were solved with Olex2^[3] using Direct Methods (ShelXS^[4a]) and refined with the ShelXL^[4b] refinement package by full-

matrix least squares on F^2 . All non-hydrogen atoms were refined anisotropically. In the structure of **3**, atom C4a was refined isotropic to yield a stable structure. The hydrogen atoms were included isotropically and treated as riding. The structure of **2b** displays three independent molecules within the asymmetric unit.

Table S1. Crystal structure and refinement data for **2a**, **2b** and **3**.

No.	2a	2b	3
Color, habit	colorless plate	colorless block	colorless block
Empirical Formula	C ₂₆ H ₃₃ BBr ₂ O ₂	C ₂₆ H ₃₃ BI ₂ O ₂	C ₃₄ H ₃₉ BO ₂ S ₂
M	548.15	642.17	554.61
Crystal system	triclinic	triclinic	triclinic
Space group	P-1	P-1	P-1
<i>a</i> /Å	9.0914(12)	10.7568(12)	9.299(3)
<i>b</i> /Å	10.6006(14)	17.0259(18)	13.239(5)
<i>c</i> /Å	14.3655(18)	22.758(2)	13.676(5)
α /°	71.643(2)	94.956(2)	97.674(8)
β /°	86.345(2)	94.394(2)	101.180(7)
γ /°	78.848(2)	103.556(2)	107.537(7)
<i>V</i> /Å ³	1289.2(3)	4016.5(7)	1541.5(10)
Z	2	8	2
μ /mm ⁻¹	3.163	2.368	0.201
T/K	100	100	100
$\theta_{\min, \max}$	2.28, 28.66	2.30, 25.32	2.37, 21.82
Completeness	0.90 to $\theta = 31.2$	0.99 to $\theta = 25.6$	0.99 to $\theta = 26.1$
Reflections: total/independent	20064/7513	45558/15014	18294/6097
<i>R</i> _{int}	0.0463	0.0386	0.0794
Final <i>R</i> 1 and <i>wR</i> 2	0.0393, 0.0644	0.0351, 0.0464	0.0661, 0.0611
Largest peak, hole/eÅ ⁻³	0.967/-0.715	1.579, -0.719	0.306, -0.401
ρ_{calc} /g cm ⁻³	1.412	1.593	1.195

NMR spectra

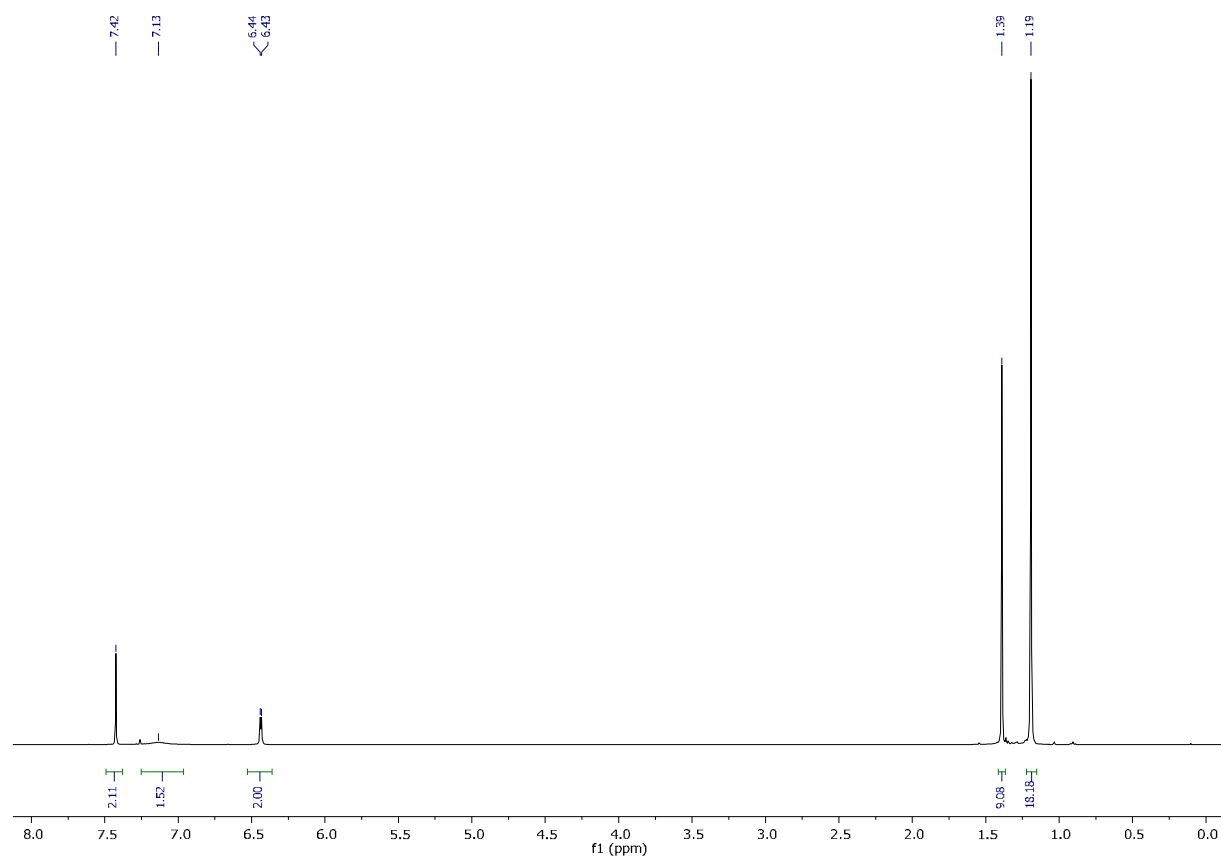


Figure S1. ^1H NMR spectrum of **2a** (in CDCl_3 , 400 MHz).

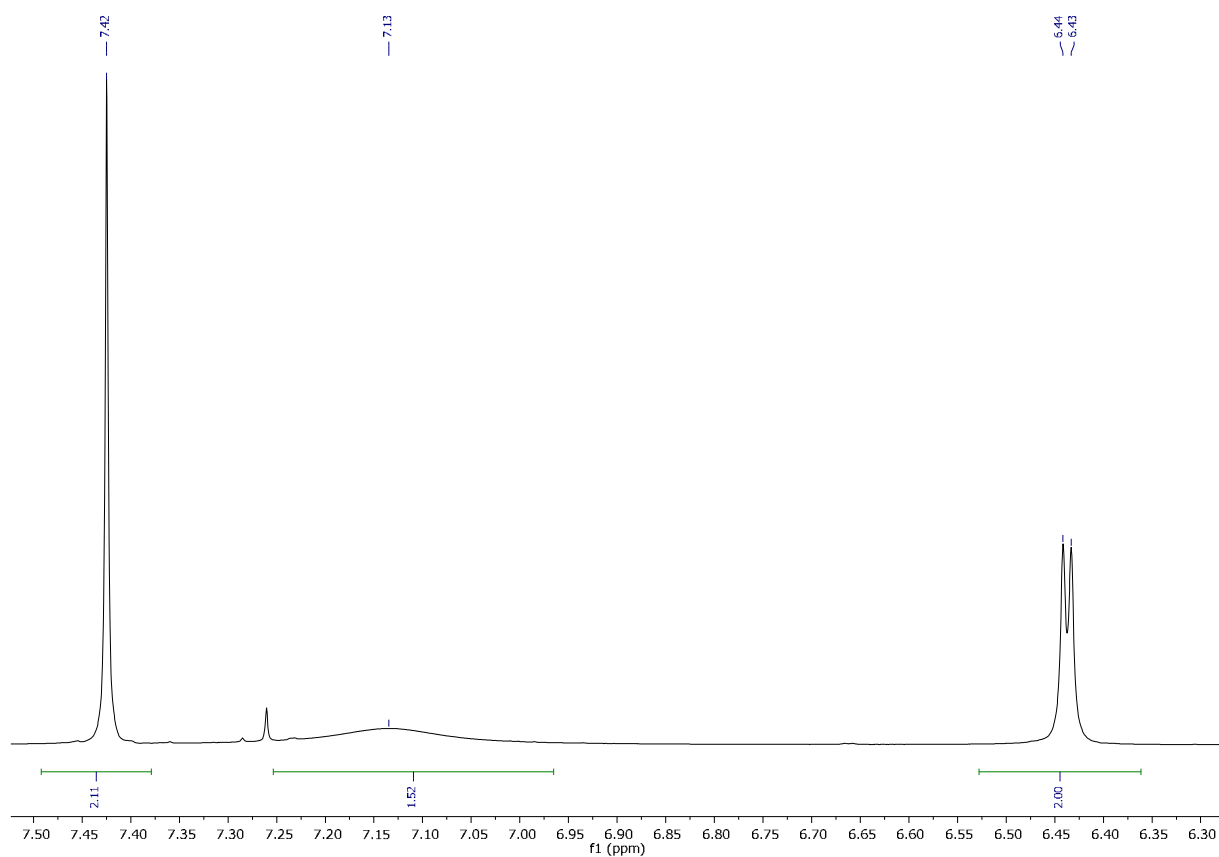


Figure S2. Detail (aromatic region) of the ^1H NMR spectrum of **2a** (in CDCl_3 , 400 MHz).

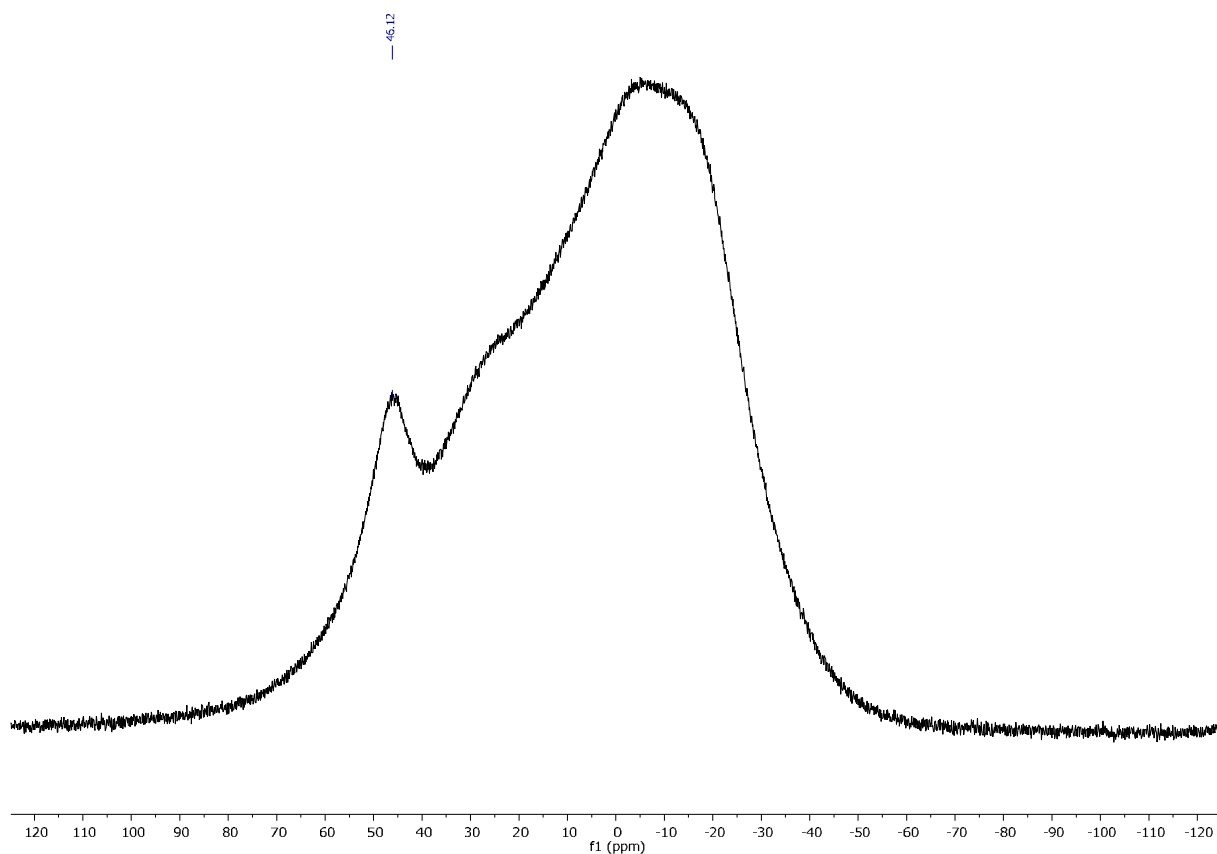


Figure S3. $^{11}\text{B}\{^1\text{H}\}$ NMR spectrum of **2a** (in CDCl_3 , 128 MHz).

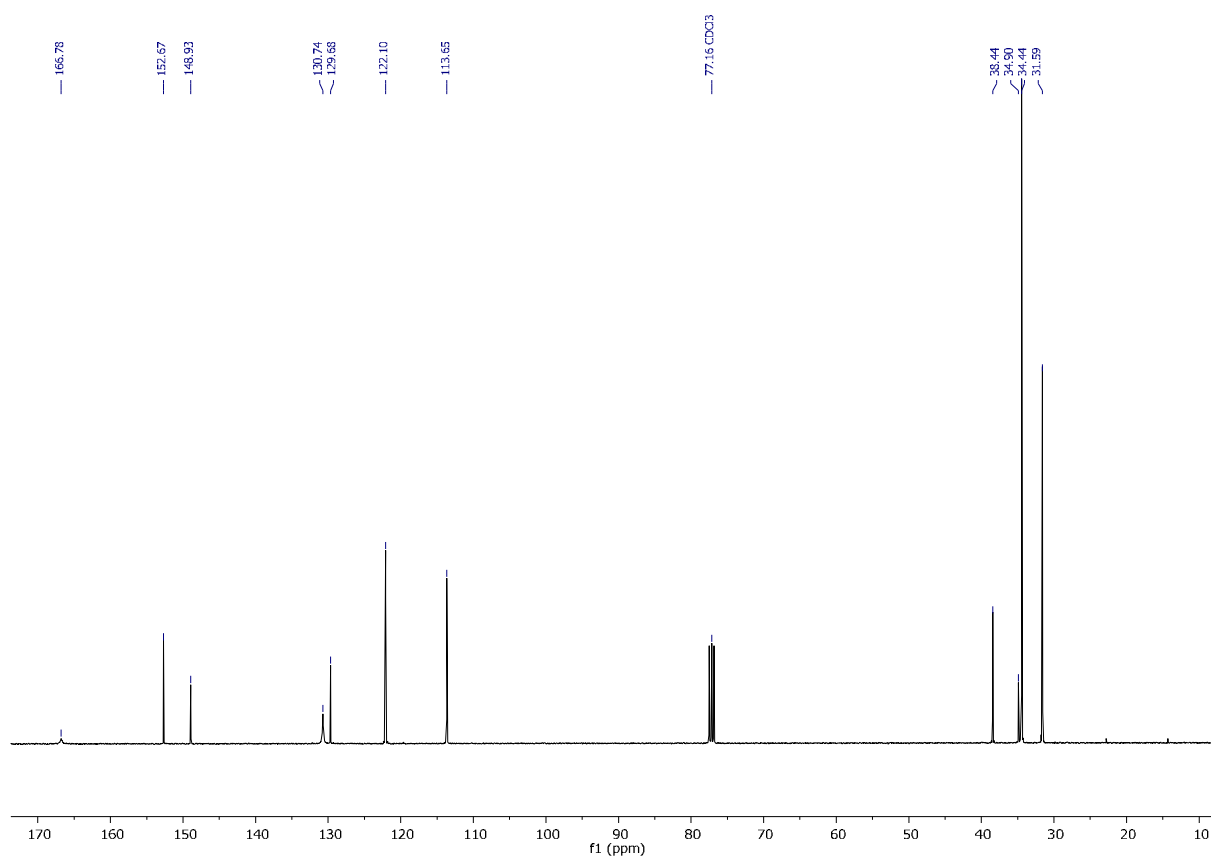


Figure S4. ¹³C NMR spectrum of **2a** (in CDCl₃, 101 MHz).

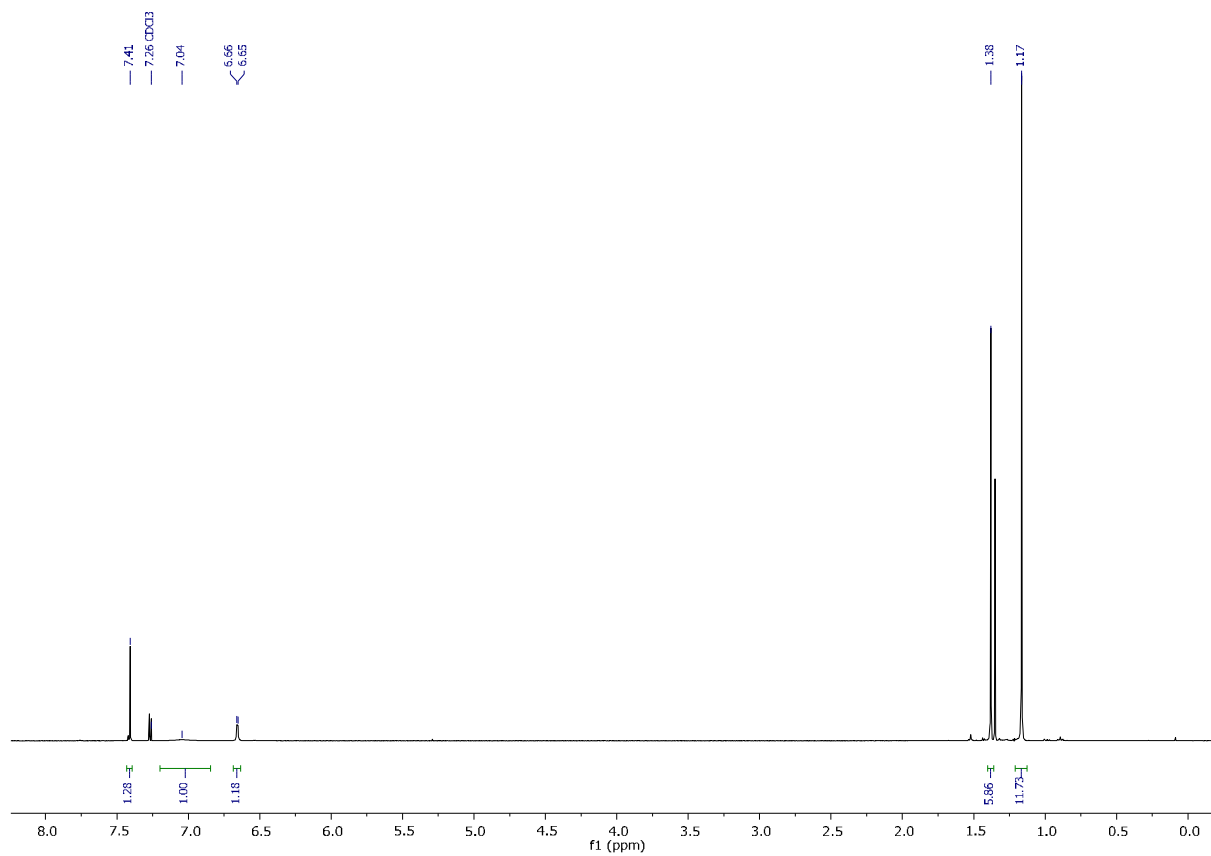


Figure S5. ¹H NMR spectrum of **2b** (in CDCl₃, 400 MHz).

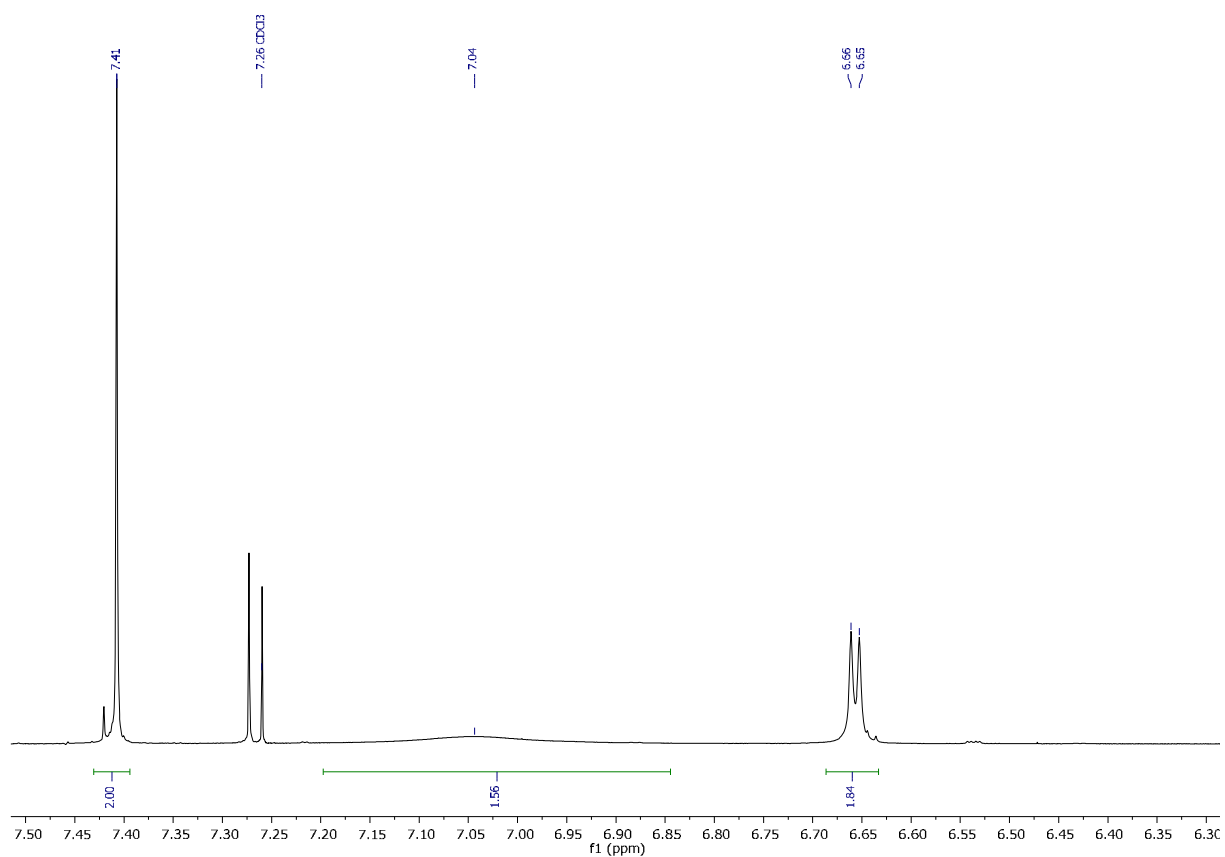


Figure S6. Detail (aromatic region) of the ^1H NMR spectrum of **2b** (in CDCl_3 , 400 MHz).

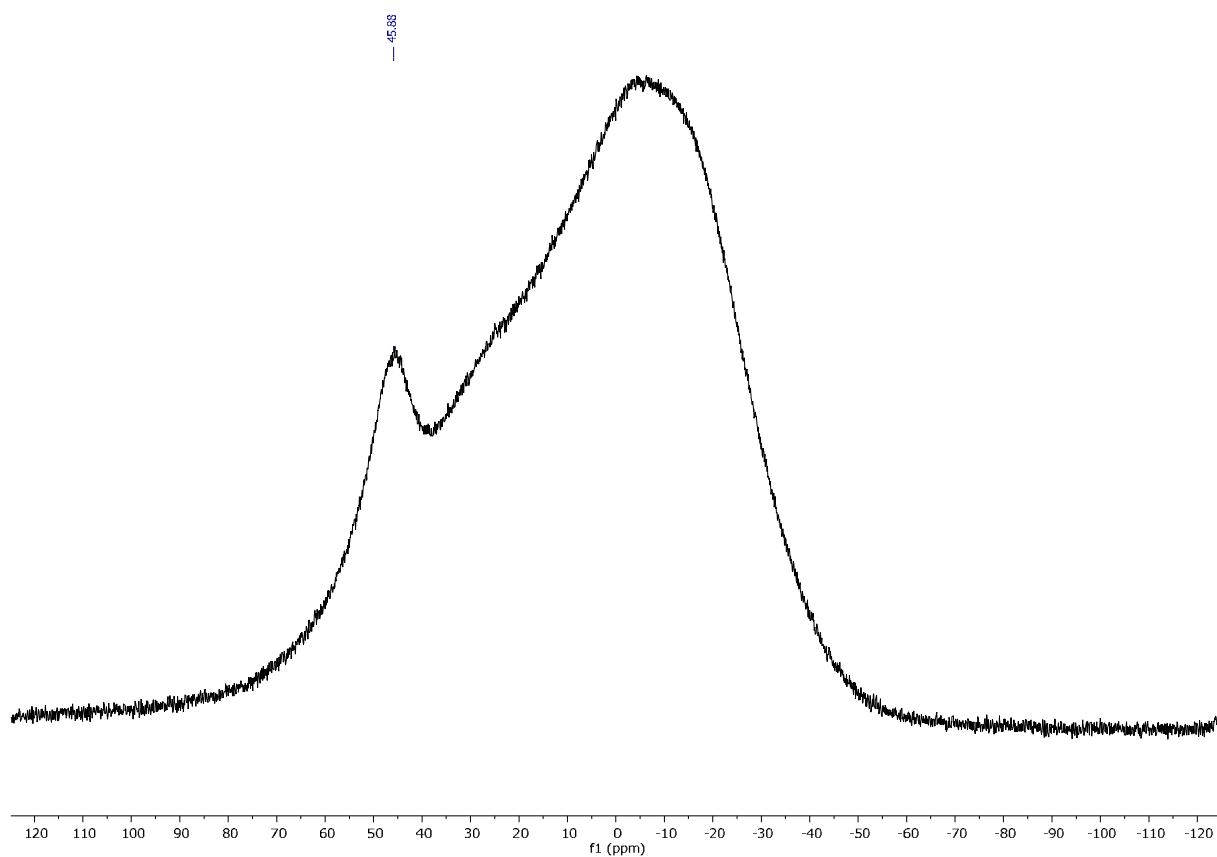


Figure S7. $^{11}\text{B}\{^1\text{H}\}$ NMR spectrum of **2b** (in CDCl_3 , 128 MHz).

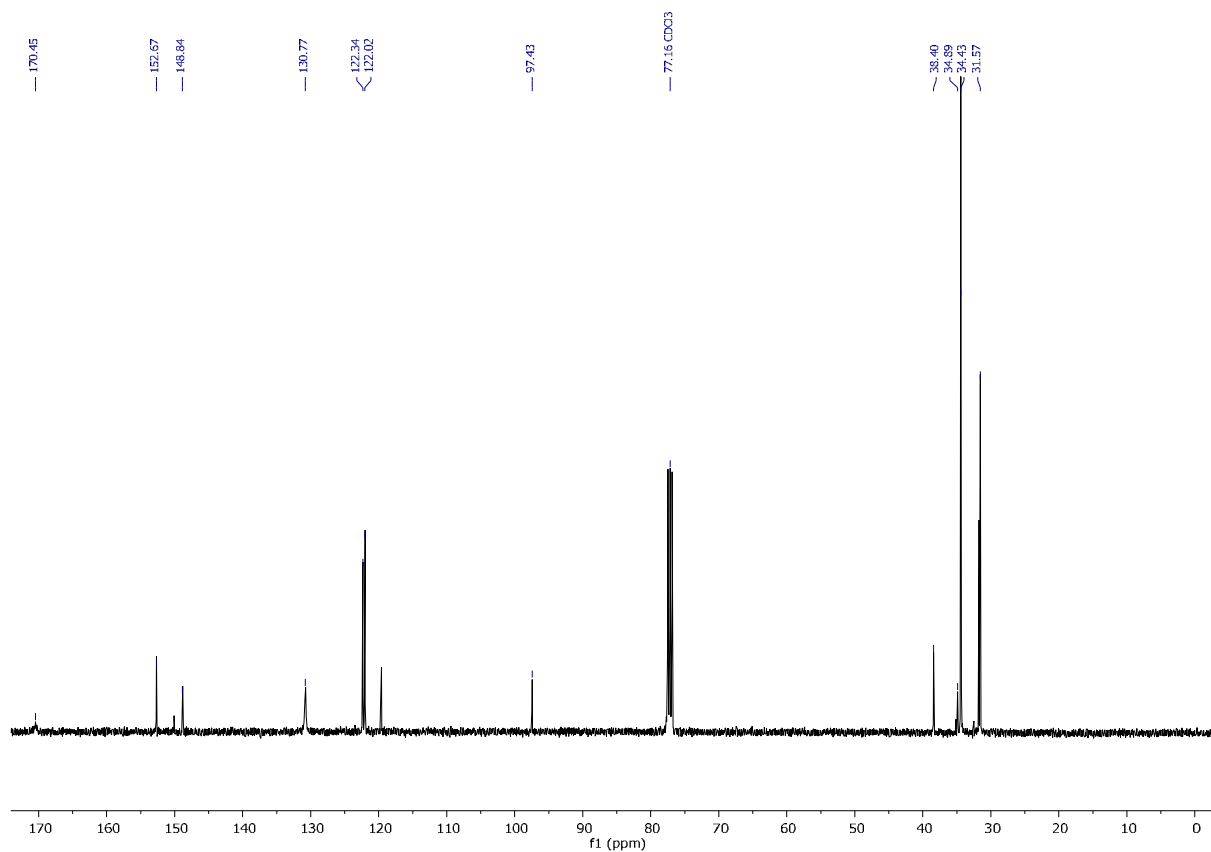


Figure S8. ¹³C NMR spectrum of **2b** (in CDCl₃, 101 MHz).

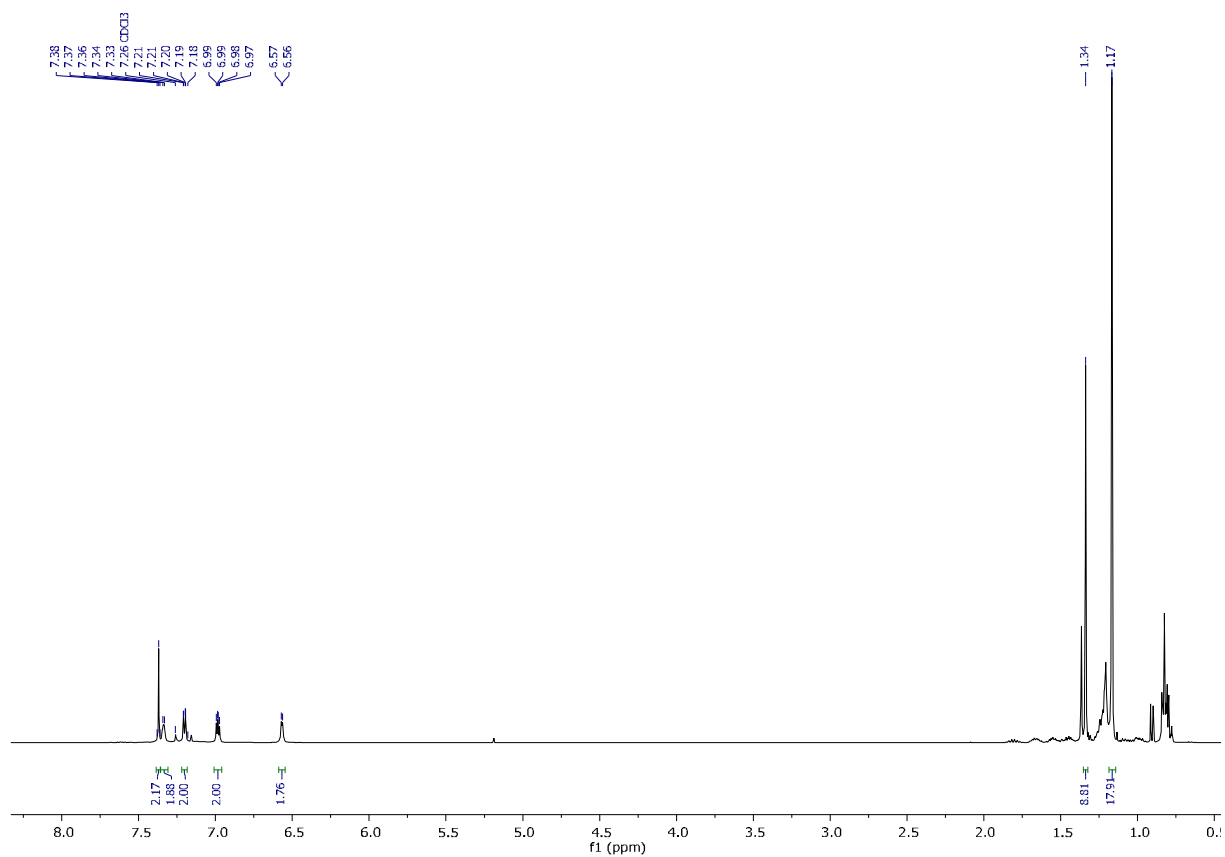


Figure S9. ¹H NMR spectrum of **3** (in CDCl₃, 400 MHz).

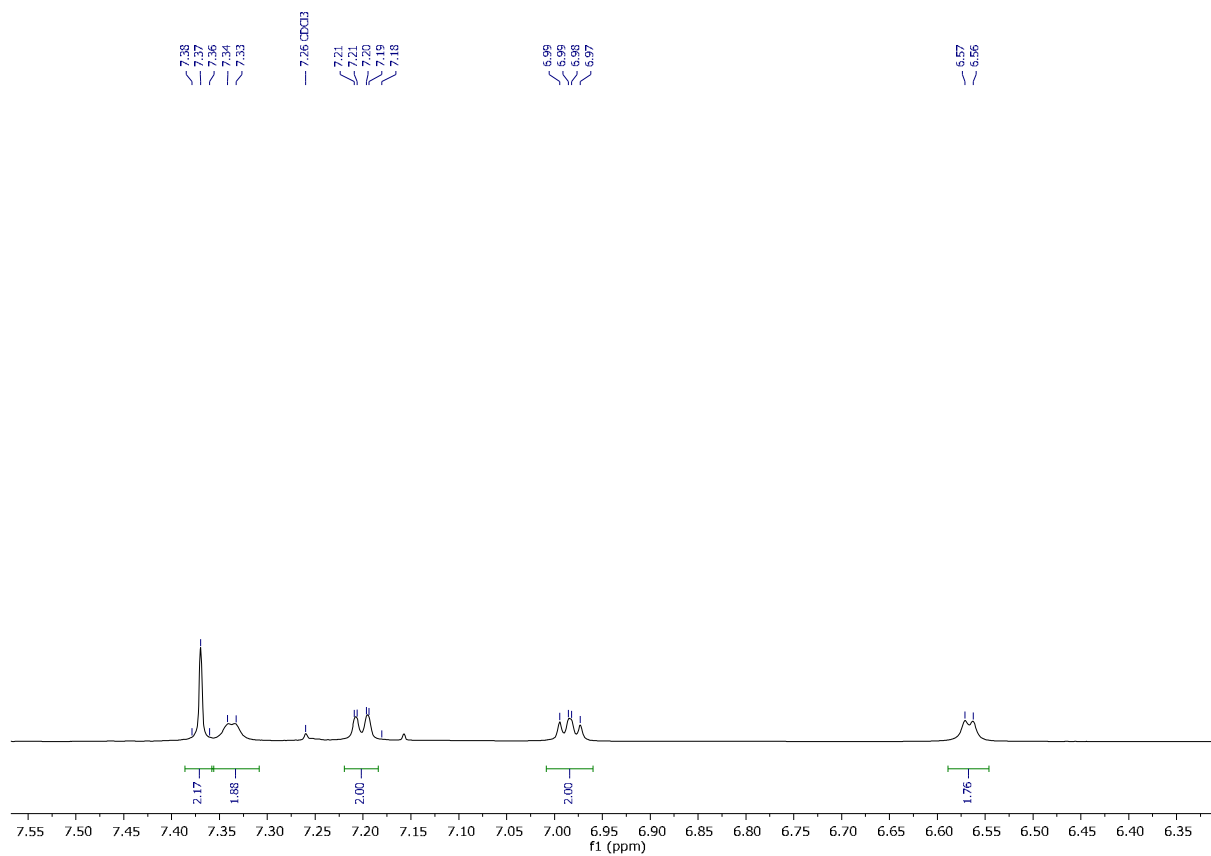


Figure S10. Detail (aromatic region) of the ^1H NMR spectrum of **3** (in CDCl_3 , 400 MHz).

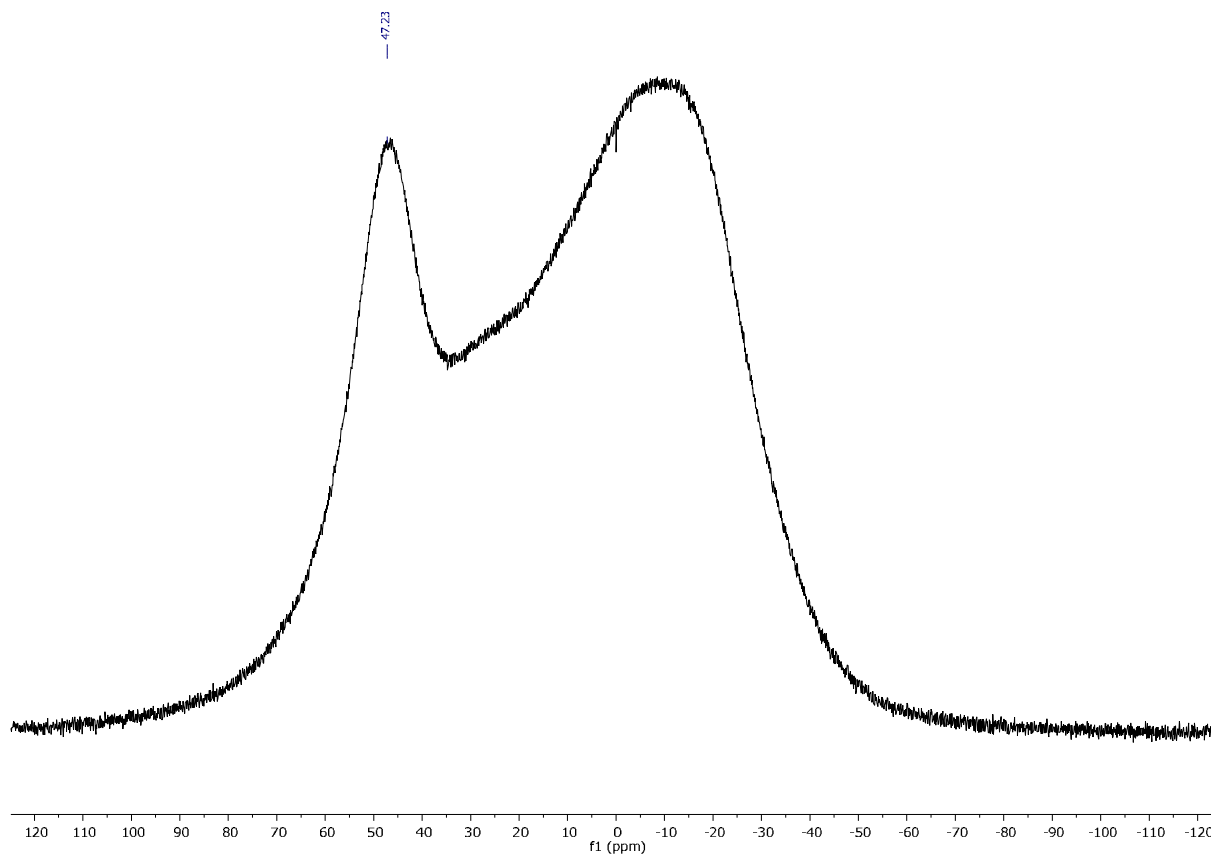


Figure S11. $^{11}\text{B}\{^1\text{H}\}$ NMR spectrum of **3** (in CDCl_3 , 128 MHz).

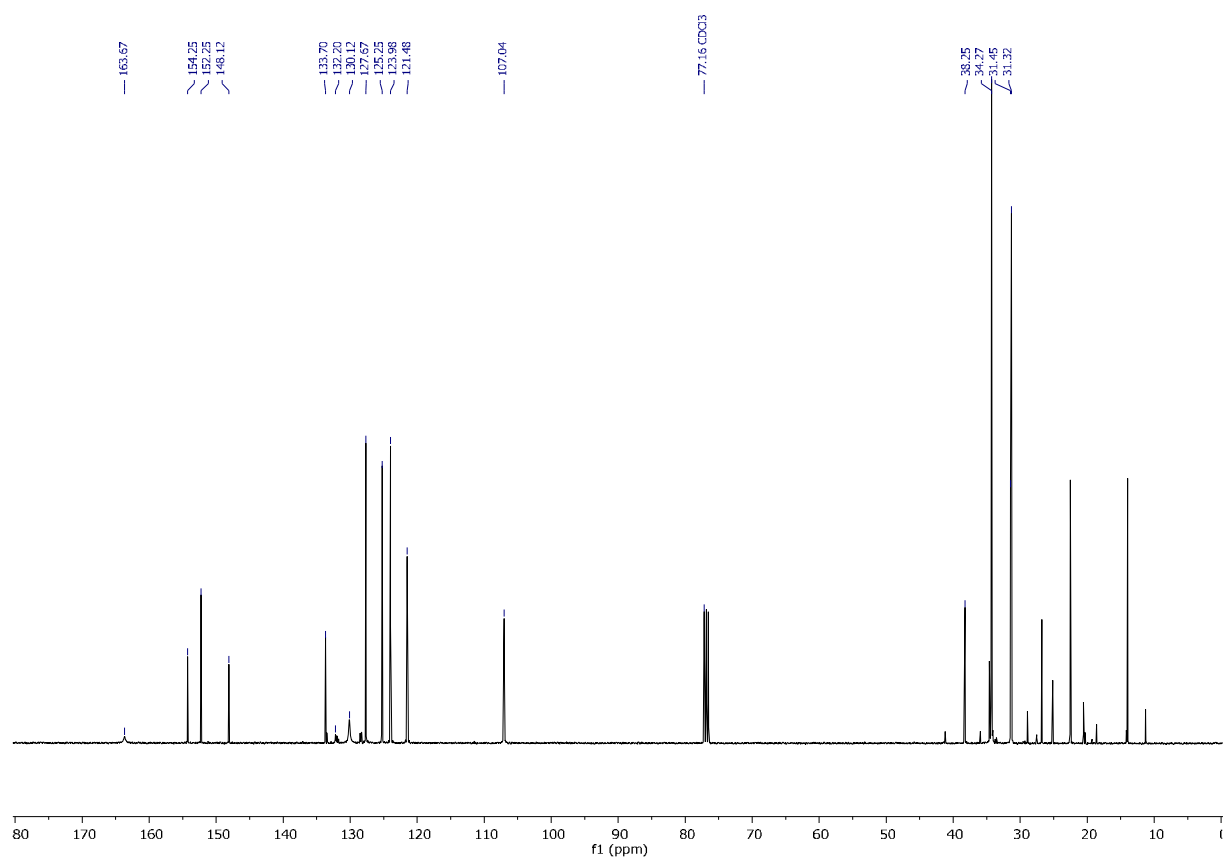


Figure S12. ¹³C NMR spectrum of **3** (in CDCl₃, 101 MHz).

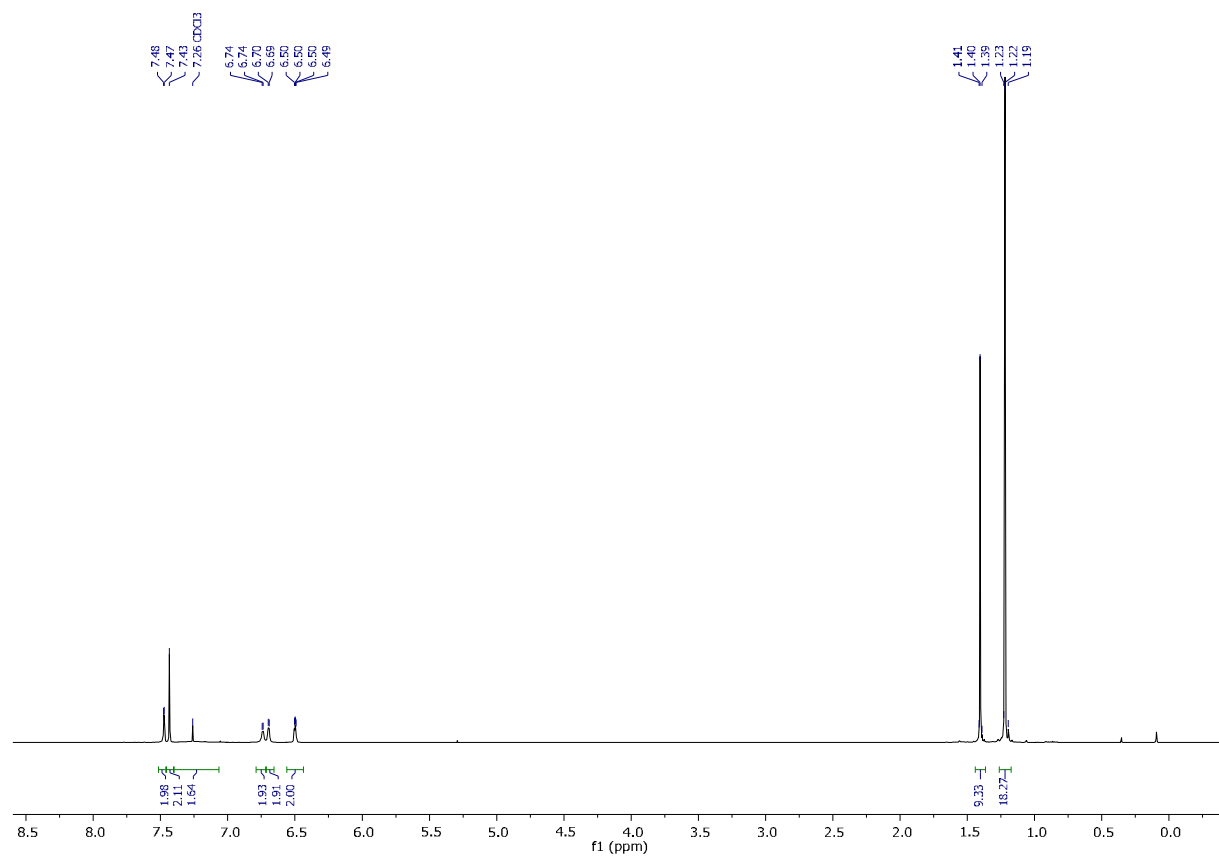


Figure S13. ¹H NMR spectrum of **4** (in CDCl₃, 400 MHz).

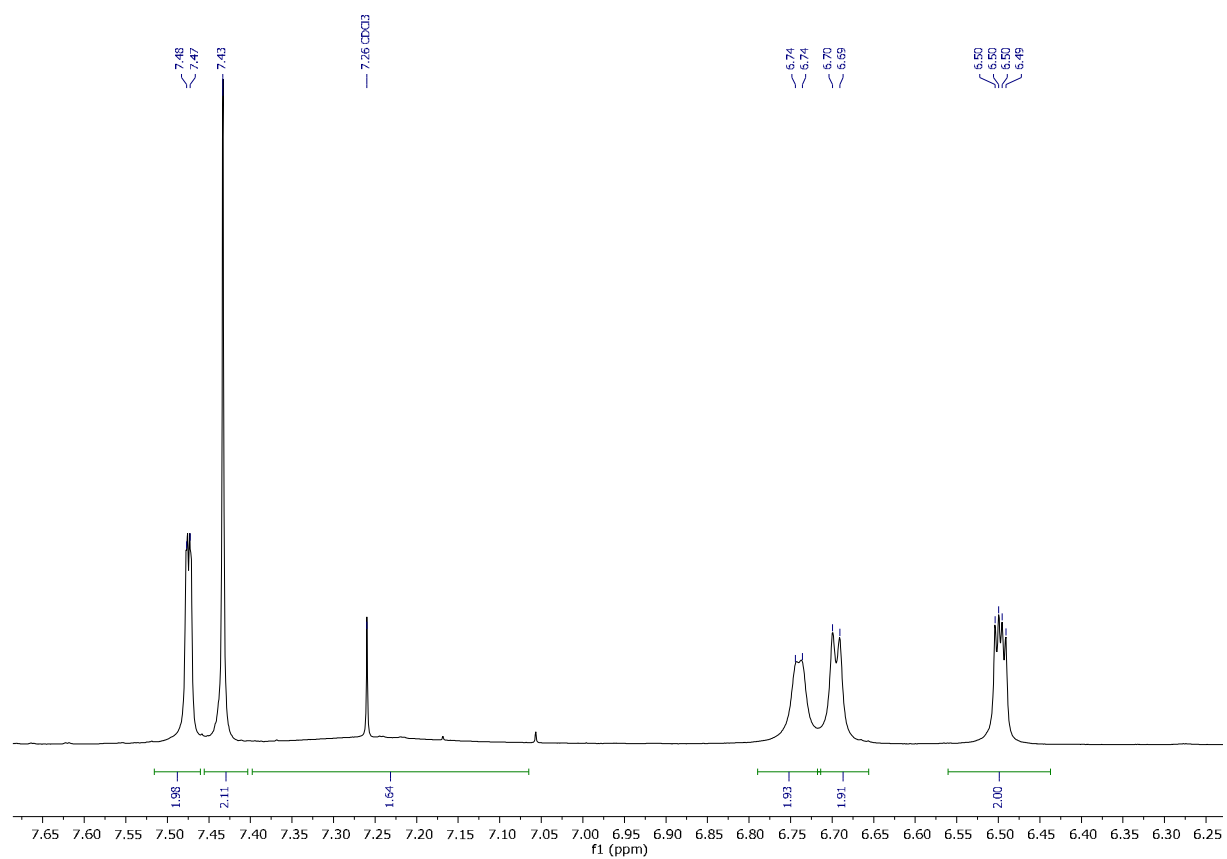


Figure S14. Detail (aromatic region) of the ^1H NMR spectrum of **4** (in CDCl_3 , 400 MHz).

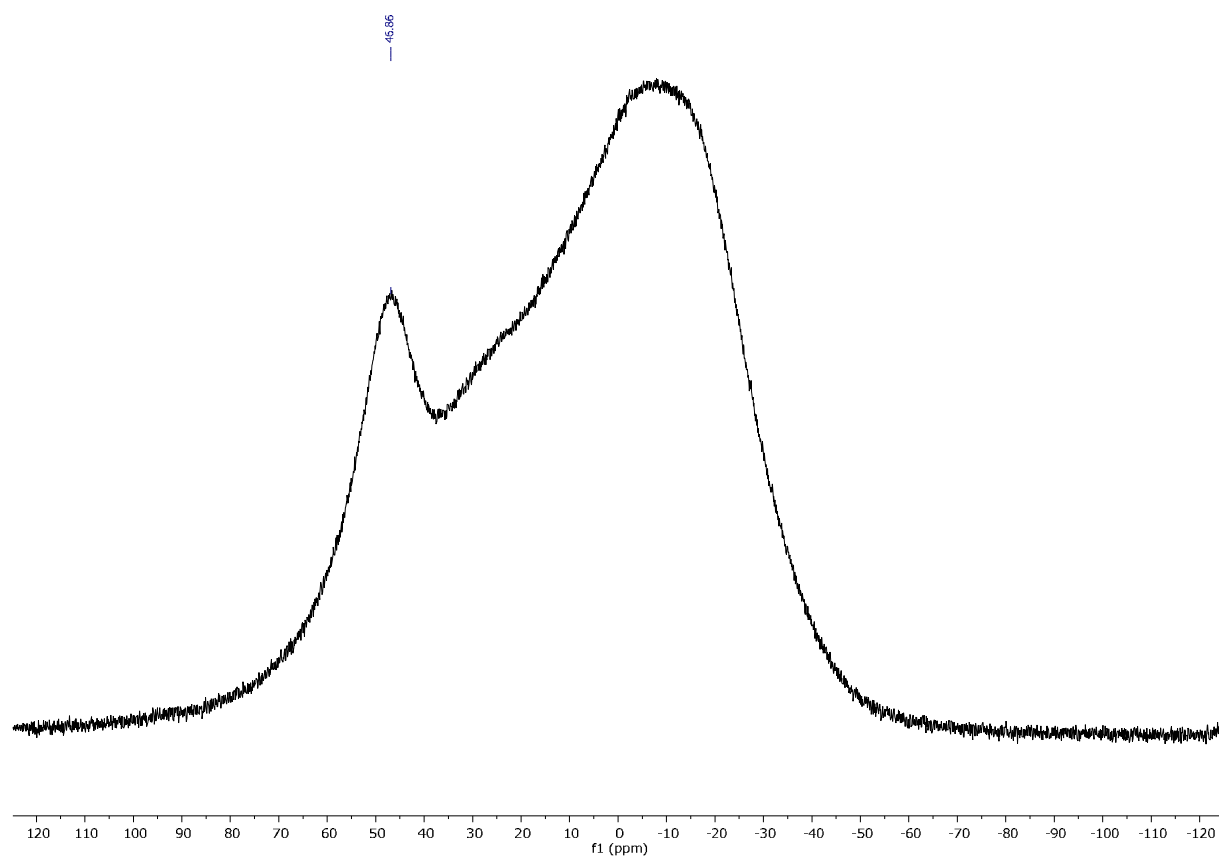


Figure S15. $^{11}\text{B}\{^1\text{H}\}$ NMR spectrum of **4** (in CDCl_3 , 128 MHz).

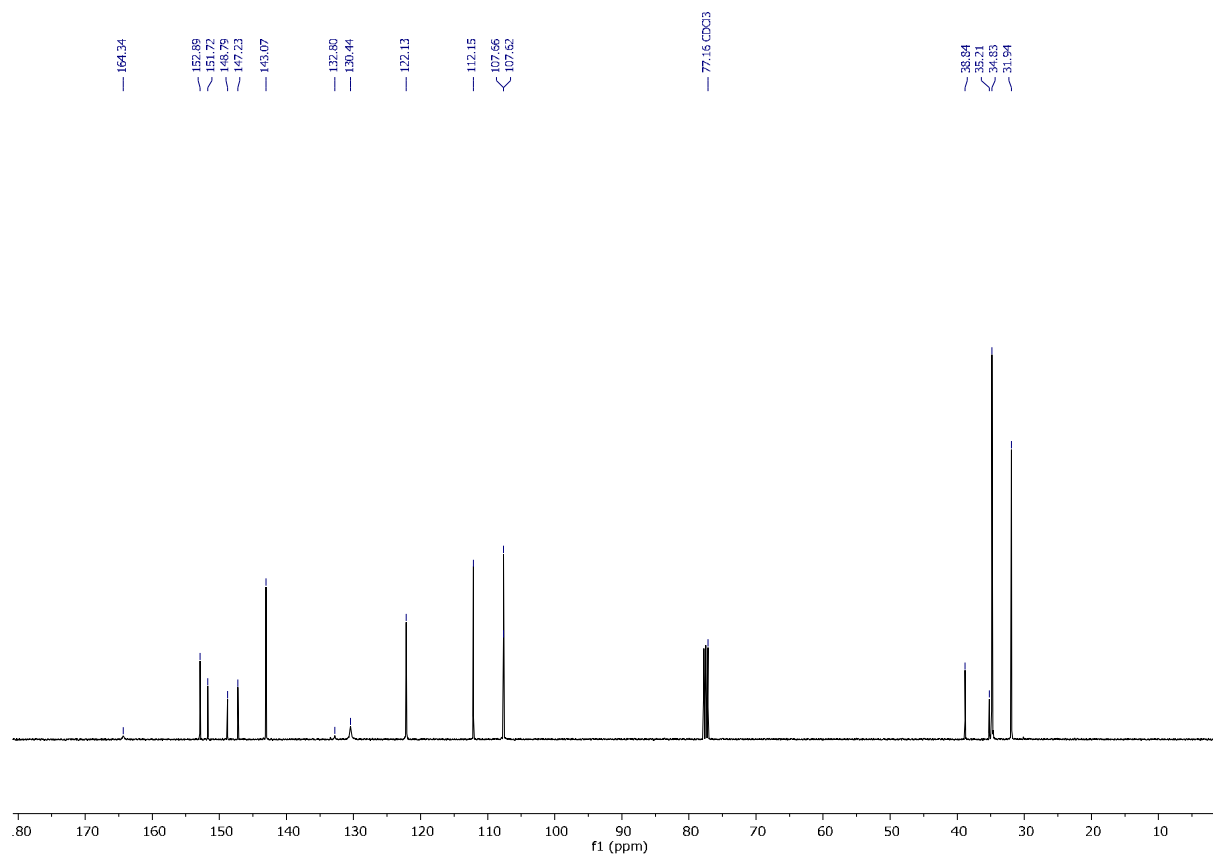


Figure S16. ^{13}C NMR spectrum of **4** (in CDCl_3 , 101 MHz).

UV-vis Spectra

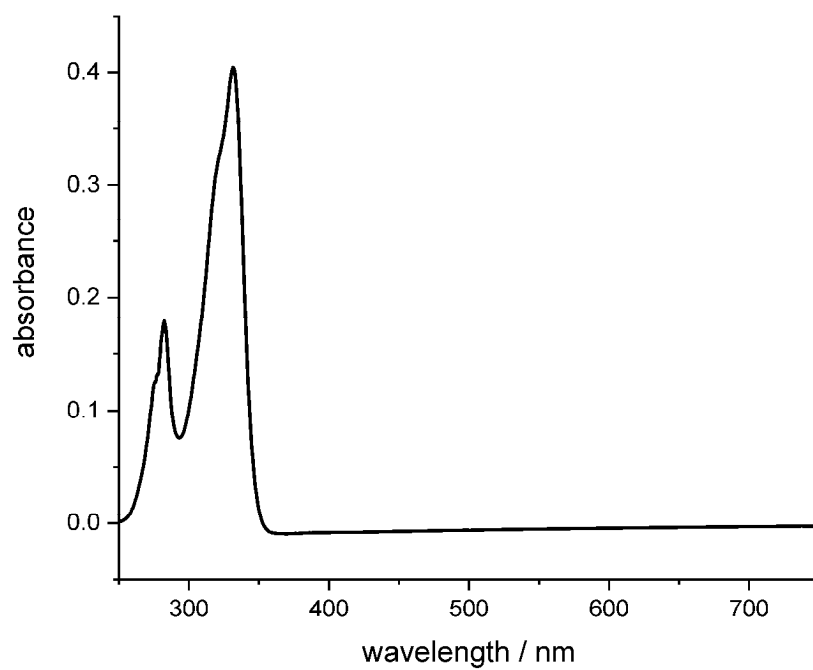


Figure S17. UV-vis spectrum of **2a** (in THF).

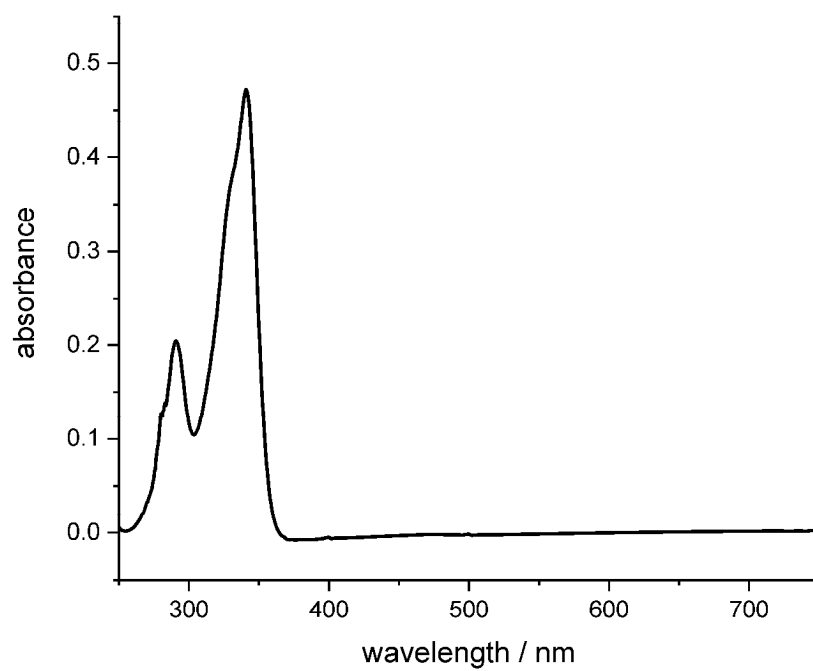


Figure S18. UV-vis spectrum of **2b** (in THF).

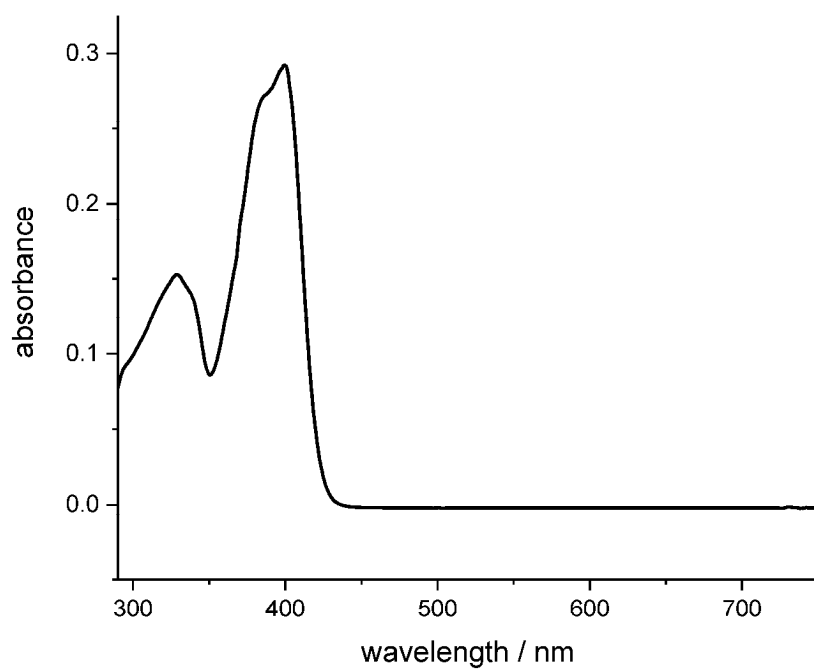


Figure S19. UV-vis spectrum of **3** (in THF).

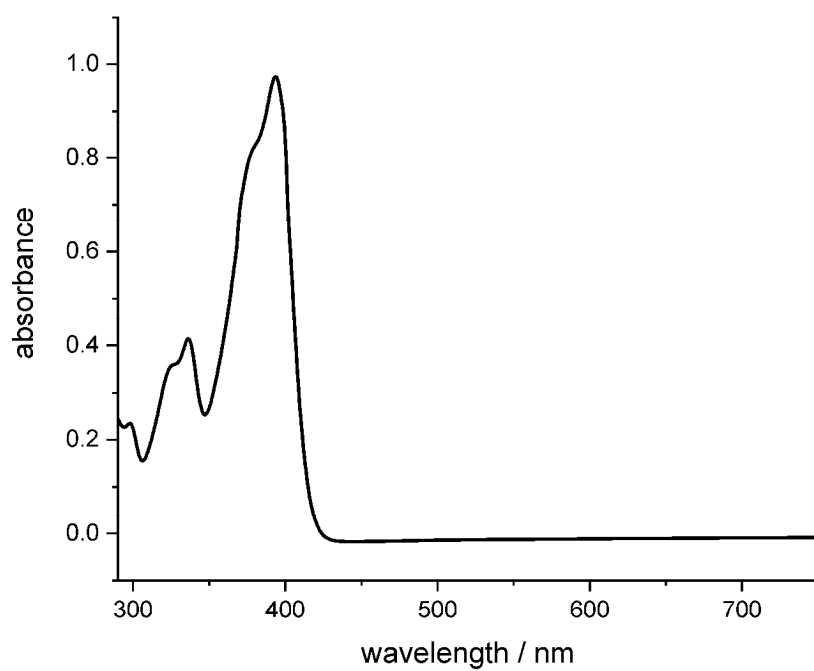


Figure 20. UV-vis spectrum of **4** (in THF).

Fluorescence spectra

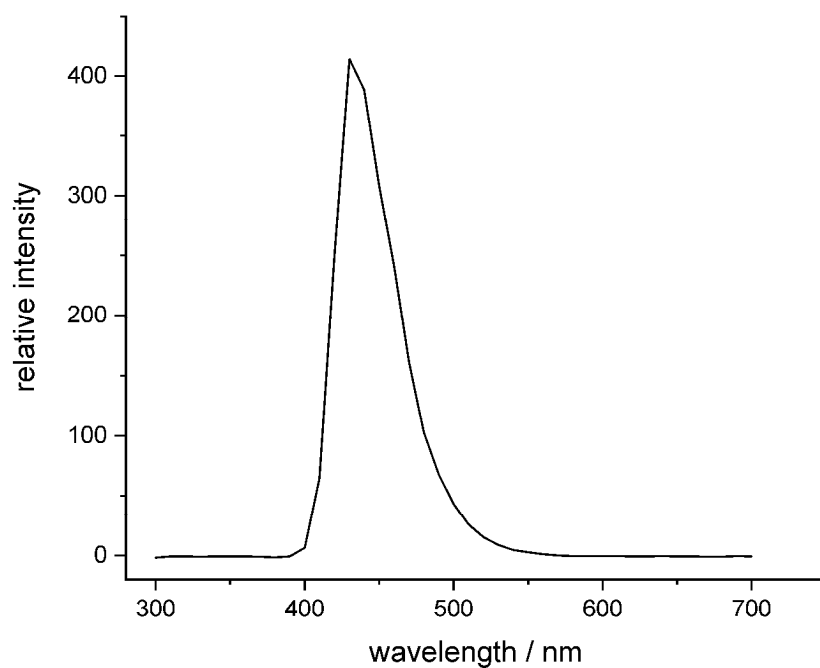


Figure S21. Fluorescence spectrum of **3** (in THF, $\lambda_{\text{ex}} = 400$ nm).

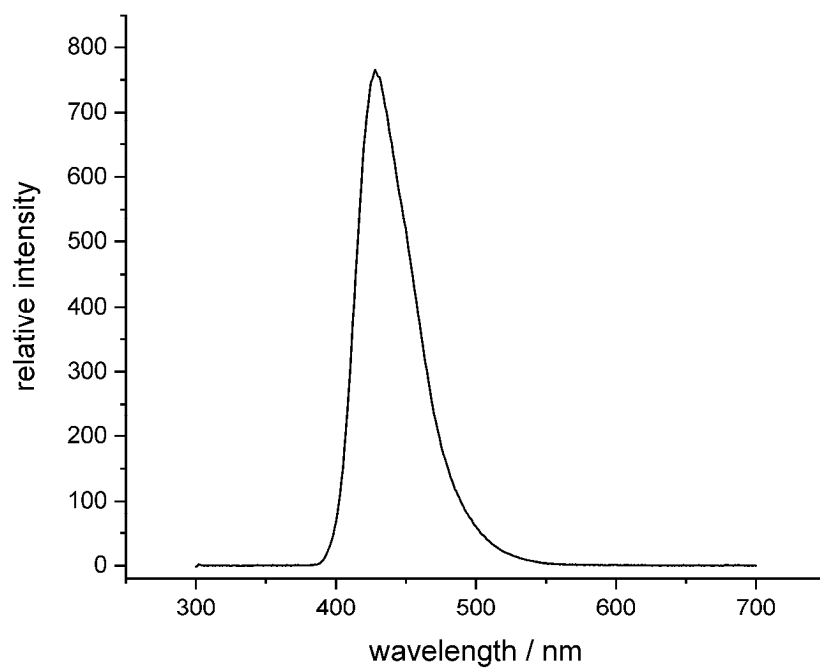


Figure S22. Fluorescence spectrum of **4** (in THF, $\lambda_{\text{ex}} = 394$ nm).

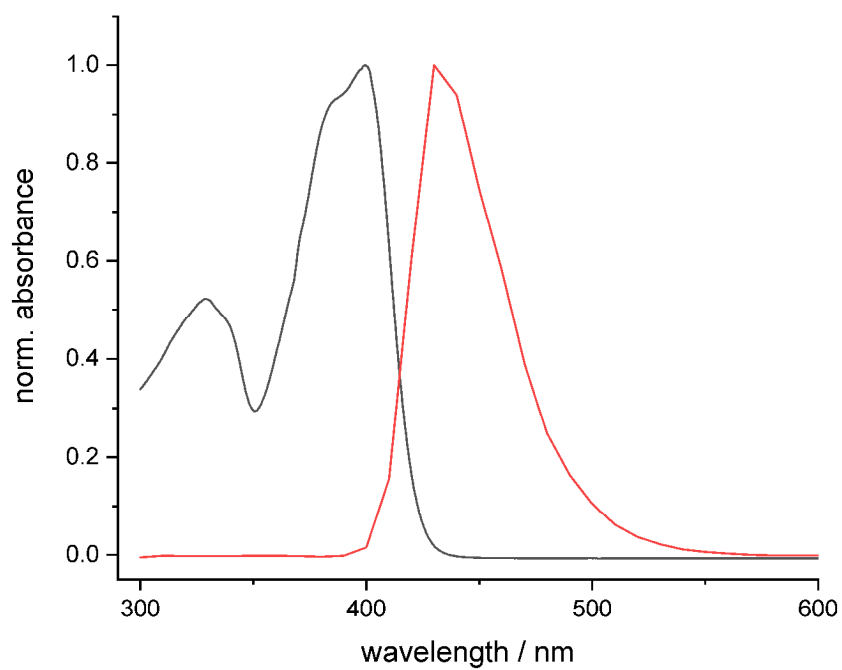


Figure S23. UV-vis (black) and fluorescence (red) spectra of **3** (in THF).

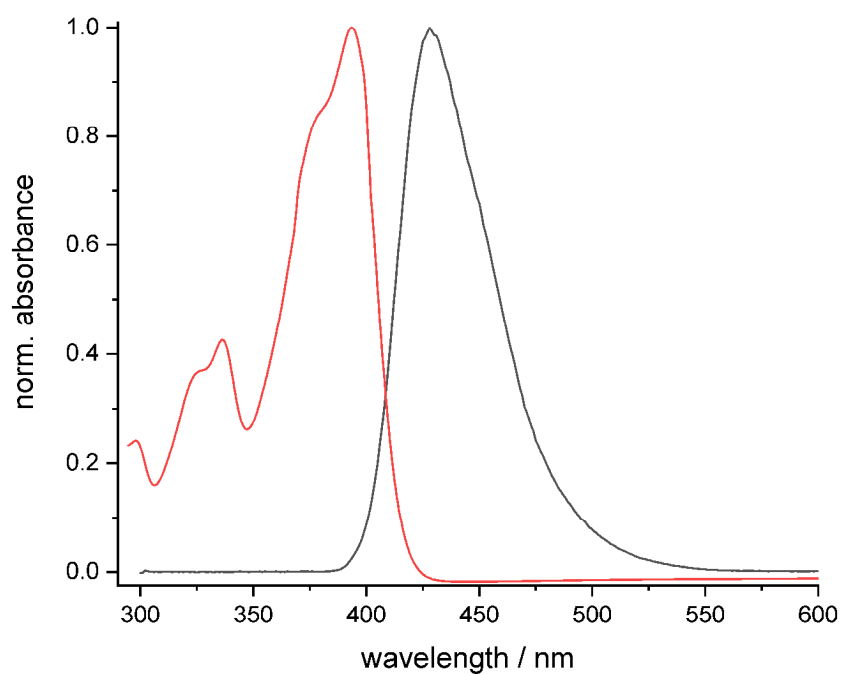


Figure S24. UV-vis (red) and fluorescence (black) spectra of **4** (in THF).

Mass spectra

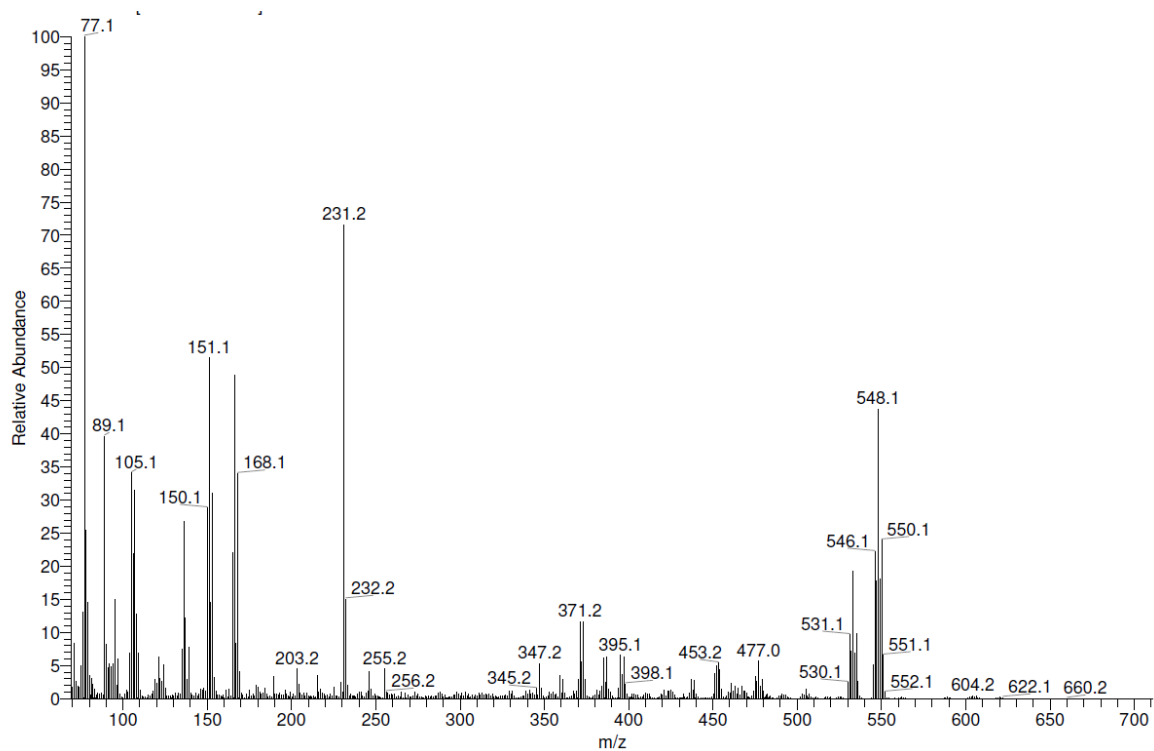


Figure S25. EI mass spectrum of 2a.

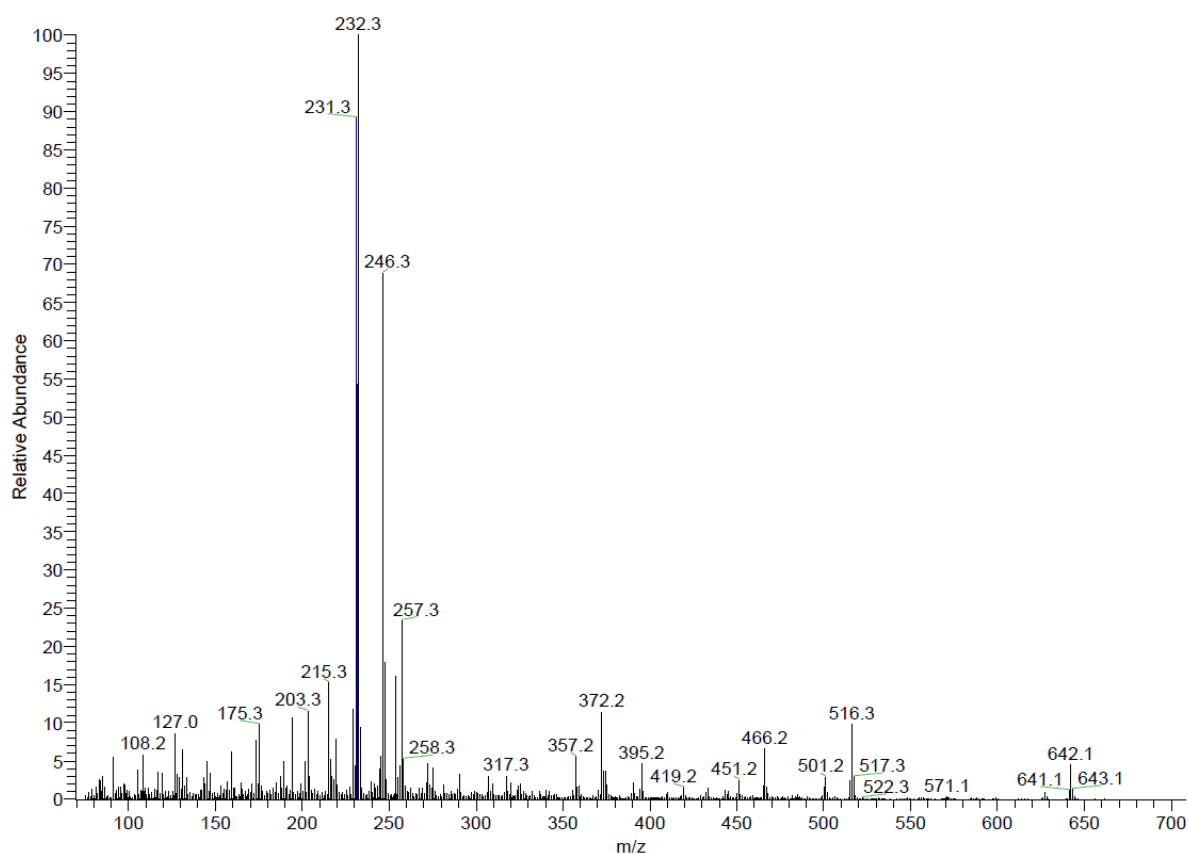


Figure S26. EI mass spectrum of 2b.

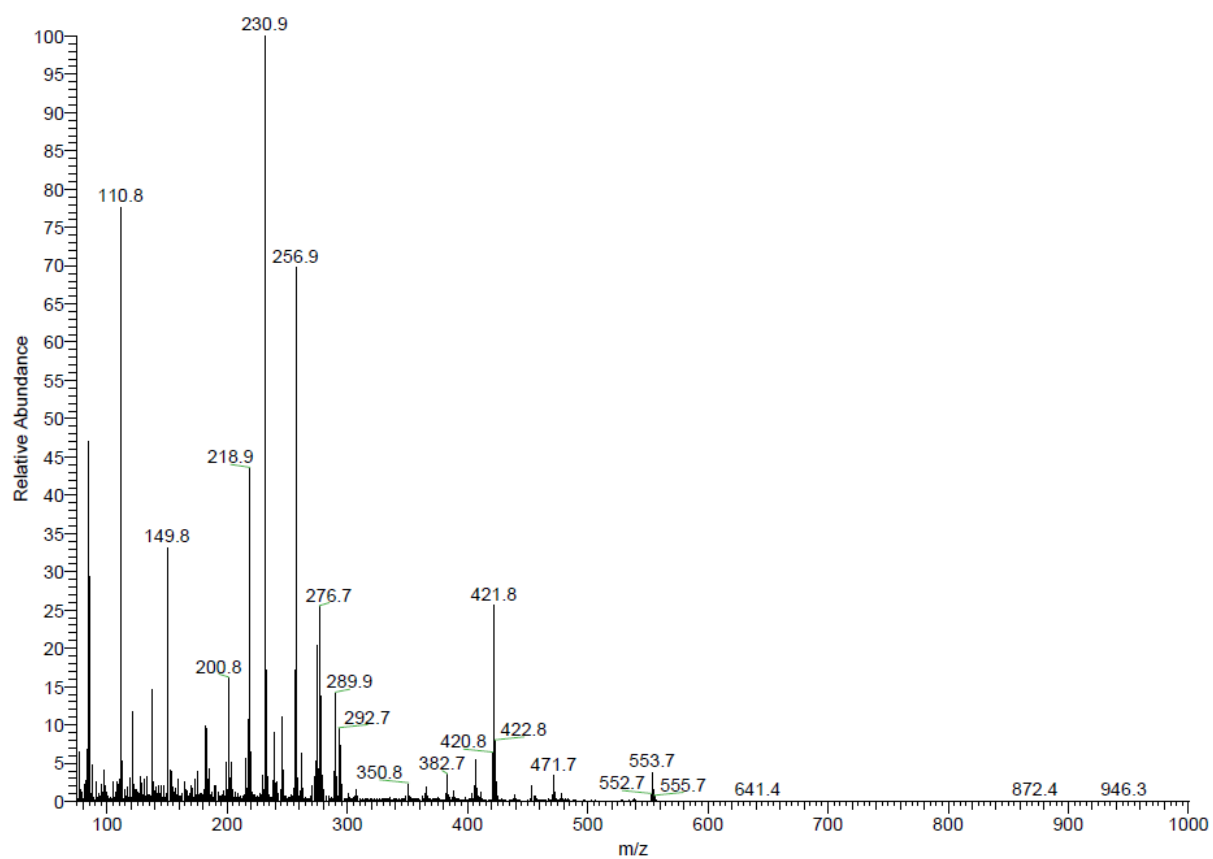


Figure S27. EI mass spectrum of 3.

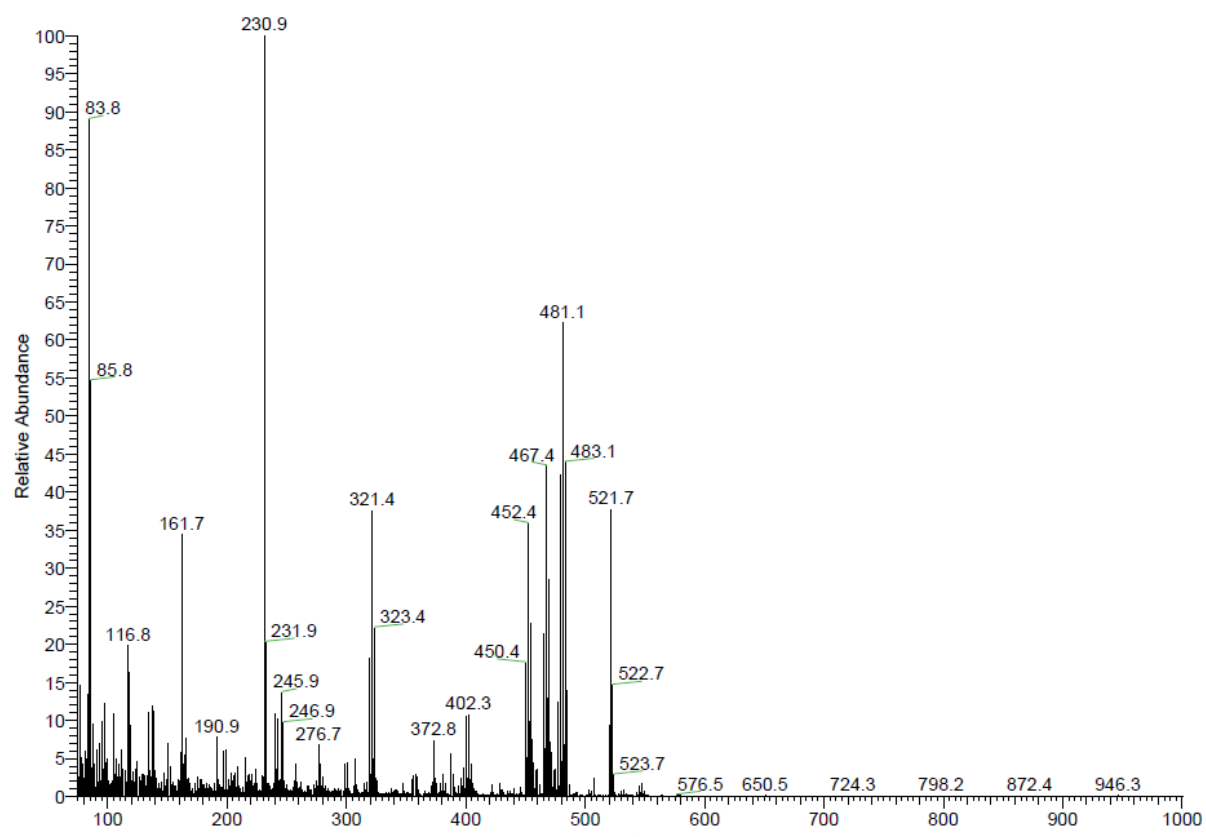


Figure S28. EI mass spectrum of 4.

Cyclic Voltammetry

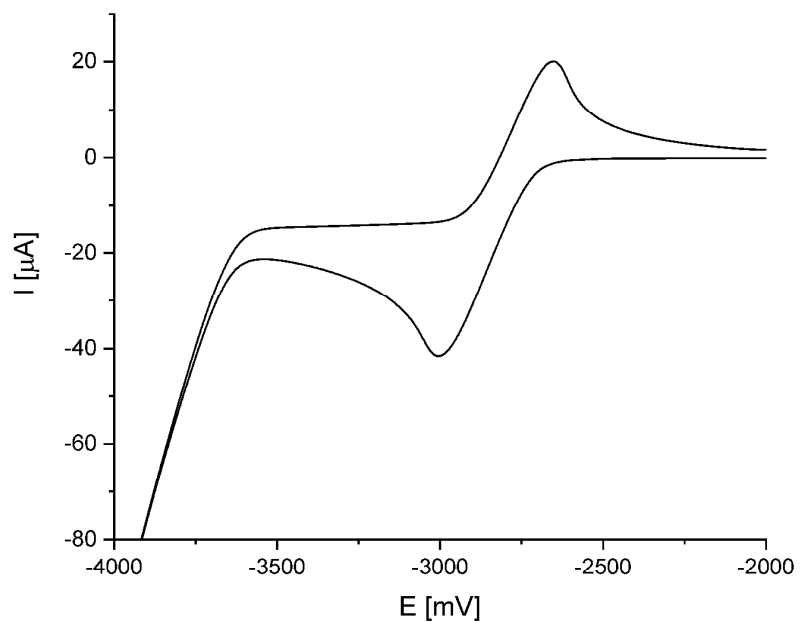


Figure 29. Cyclic voltammogram of **1** in THF ($1 \cdot 10^{-3} \text{ M}$), recorded vs the ferrocene/ferrocenium couple as internal standard (scan rate: 100 mV s^{-1}).

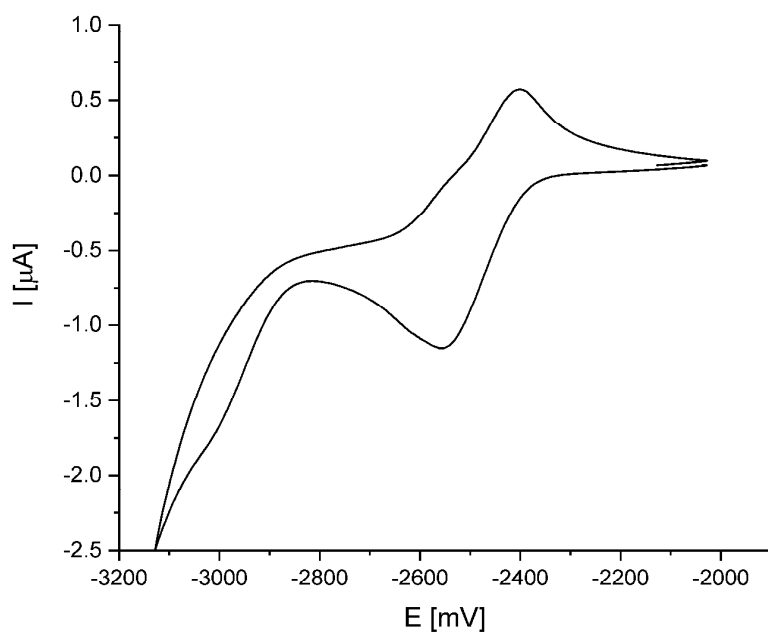


Figure S30. Cyclic voltammogram of **3** in THF ($1 \cdot 10^{-3} \text{ M}$), recorded vs the ferrocene/ferrocenium couple as internal standard (scan rate: 100 mV s^{-1}).

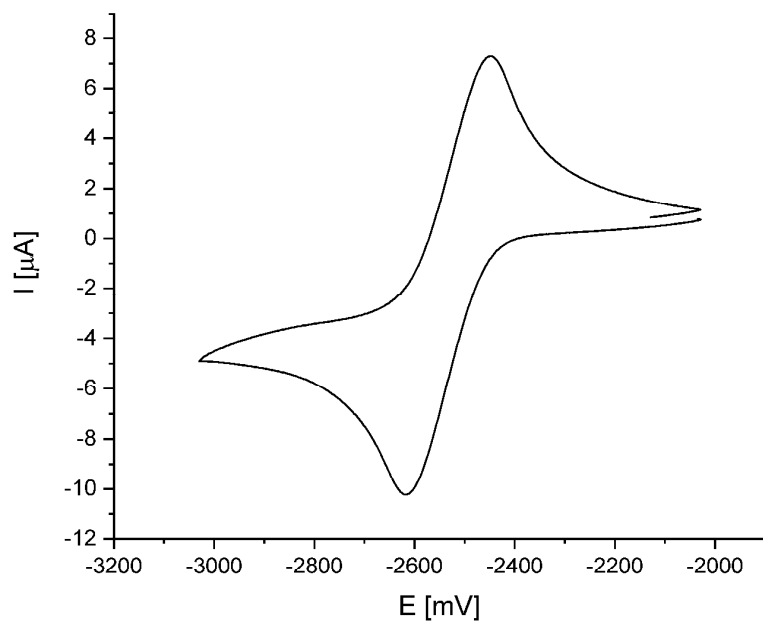


Figure S31. Cyclic voltammogram of **4** in THF ($1 \cdot 10^{-3}$ M), recorded vs the ferrocene/ferrocenium couple as internal standard (scan rate: 100 mV s^{-1}).

2 Computational Information

Computational methods. DFT calculations were carried out with the TURBOMOLE V7.0.1 program package.^[5] Optimizations were performed with Becke's three parameter exchange-correlation hybrid functional B3LYP^[6] in combination with the valence-double- ζ basis set def2-SV(P).^[7] The empirical dispersion correction DFT-D3 by Grimme was used including the three-body term and with Becke-Johnson (BJ) damping.^[8] The stationary points were characterized as minima by analytical vibrational frequency calculations.^[9] Vertical singlet excitations were calculated by means of time-dependent DFT^[10] using the same density functional–basis set combination as specified above.

Table S2. Results from TD-DFT calculations (π – π^* excitation marked in bold).

Compound	No.	λ / nm	Oscillator strength f	Orbital contributions	$ c ^2$ / %
2a'	1	382.6	0.0108	HOMO \rightarrow LUMO	99.3
	2	355.5	0.0031	HOMO–2 \rightarrow LUMO	93.7
	3	330.6	0.5918	HOMO–1 \rightarrow LUMO	93.1
2b'	1	384.3	0.0126	HOMO \rightarrow LUMO	95.7
	2	356.9	0.0063	HOMO–2 \rightarrow LUMO	95.1
	3	339.6	0.6164	HOMO–1 \rightarrow LUMO	91.1
5	1	404.8	1.2140	HOMO \rightarrow LUMO	99.4
3'	1	418.1	0.9106	HOMO \rightarrow LUMO	99.4
	2	397.3	0.0201	HOMO–1 \rightarrow LUMO	81.0
				HOMO–2 \rightarrow LUMO	17.3
	3	367.7	0.0015	HOMO–3 \rightarrow LUMO	97.1
	5	308.3	0.2994	HOMO \rightarrow LUMO+1	78.4
			HOMO–2 \rightarrow LUMO	14.9	
6	1	384.6	1.2270	HOMO \rightarrow LUMO	99.5
4'	1	410.6	0.8855	HOMO \rightarrow LUMO	99.4
	2	390.9	0.0176	HOMO–1 \rightarrow LUMO	61.6
				HOMO–2 \rightarrow LUMO	37.2
	3	361.5	0.0014	HOMO–3 \rightarrow LUMO	98.7
	5	287.7	0.3086	HOMO \rightarrow LUMO+1	87.2
			HOMO–2 \rightarrow LUMO	5.8	

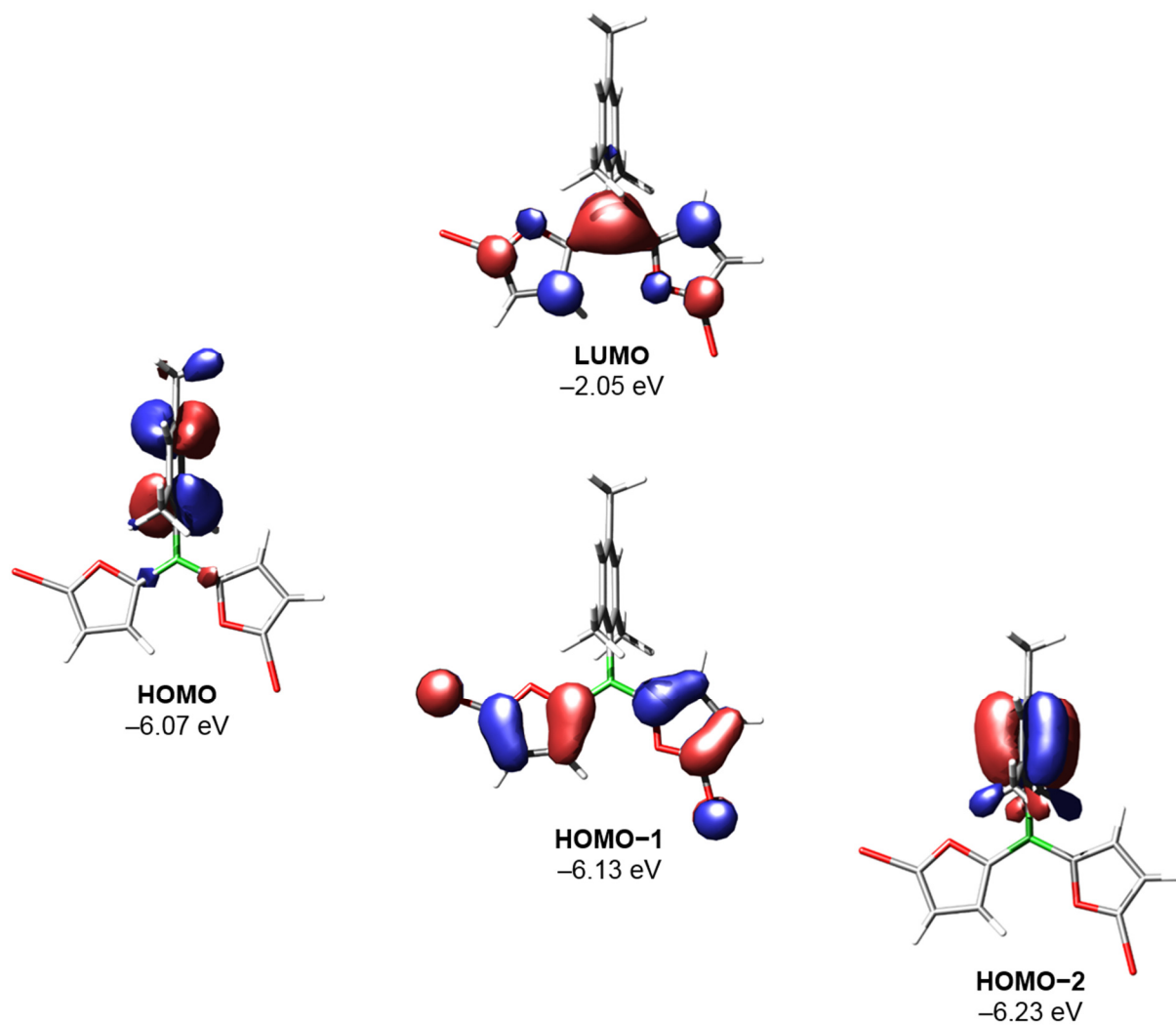


Figure S32. Calculated frontier orbitals of **2a'** (isovalue 0.04 a.u.).

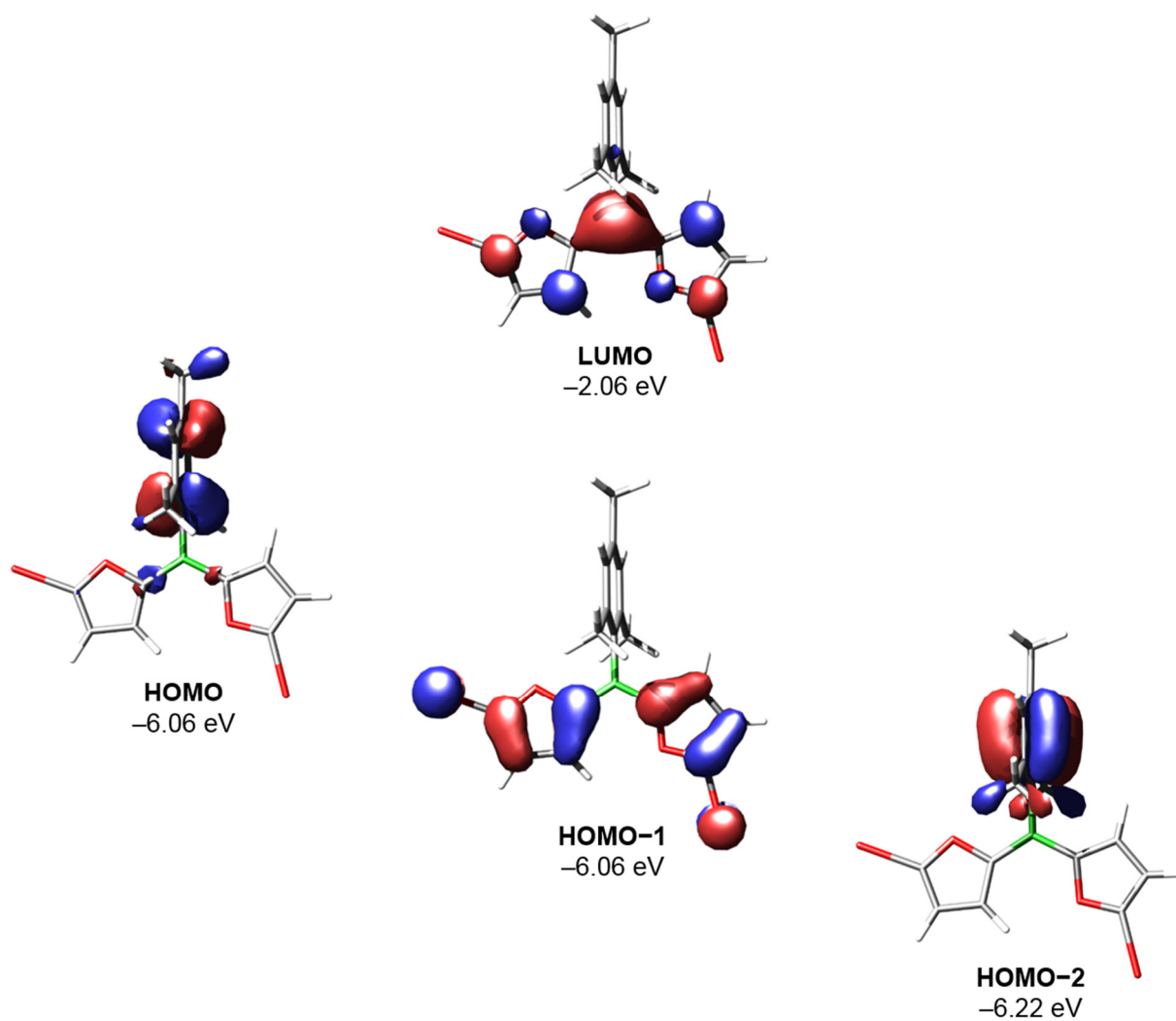


Figure S33. Calculated frontier orbitals of **2b'** (isovalue 0.04 a.u.).

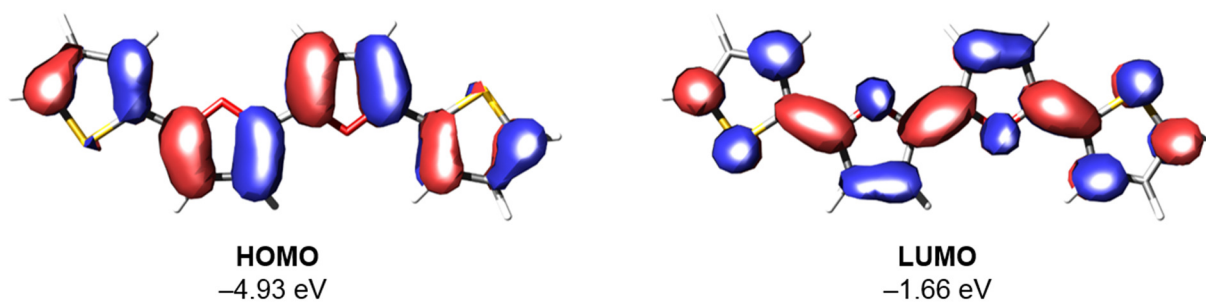


Figure S34. Calculated frontier orbitals of **5** (isovalue 0.03 a.u.).

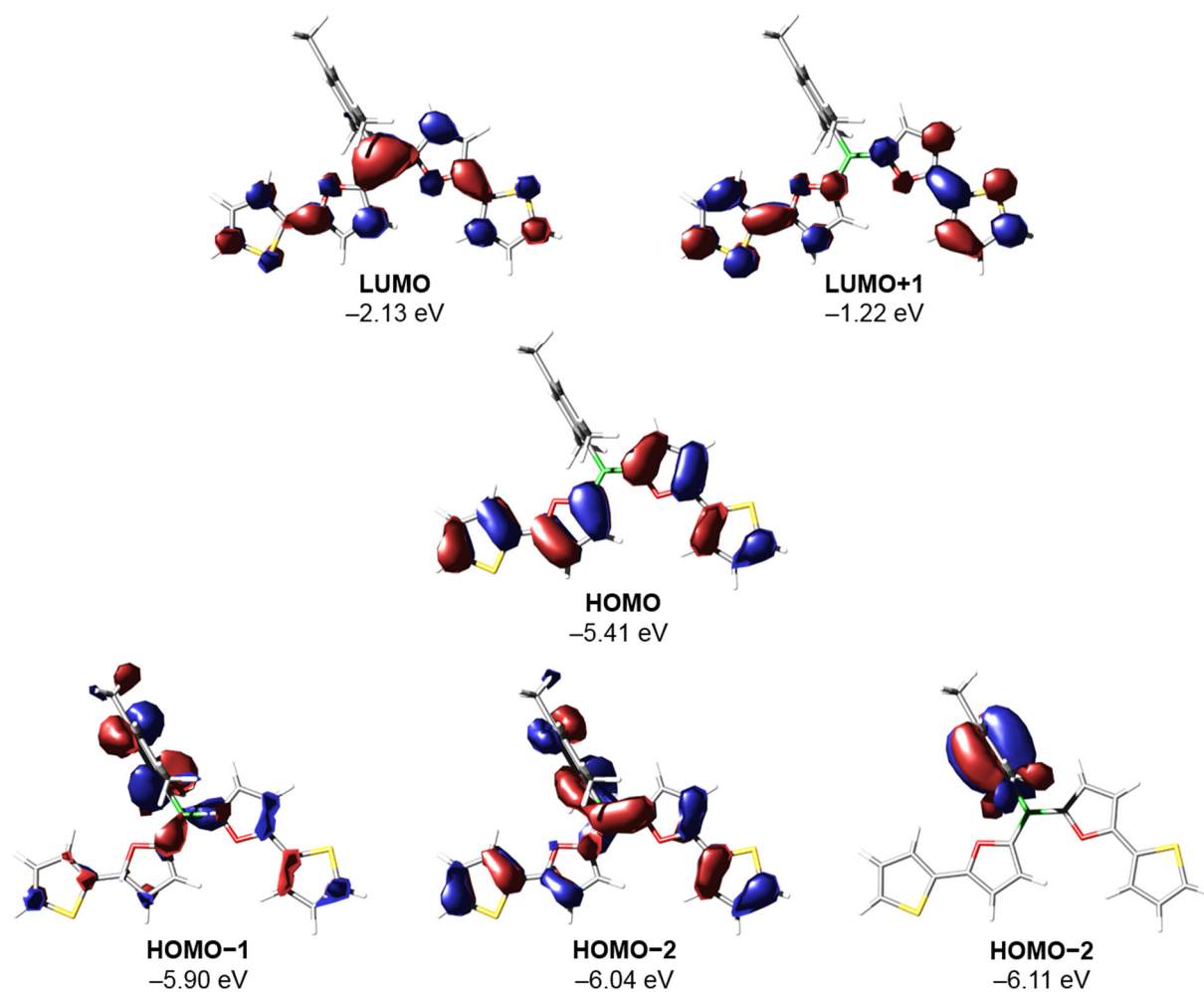


Figure S35. Calculated frontier orbitals of **3'** (isovalue 0.03 a.u.).

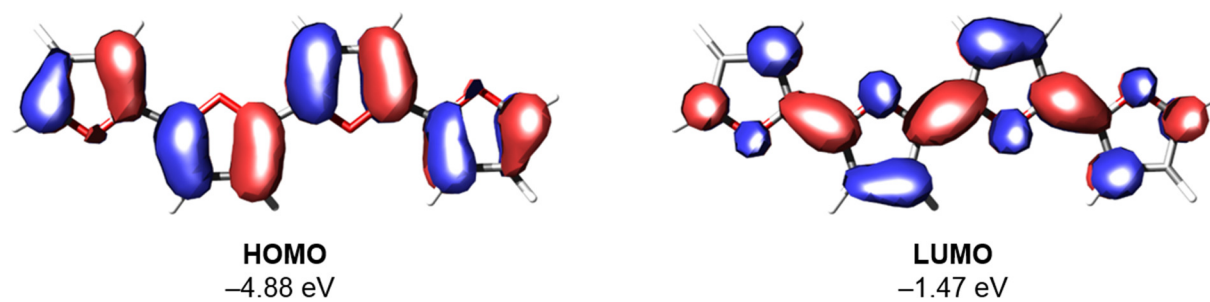


Figure S36. Calculated frontier orbitals of **6** (isovalue 0.03 a.u.).

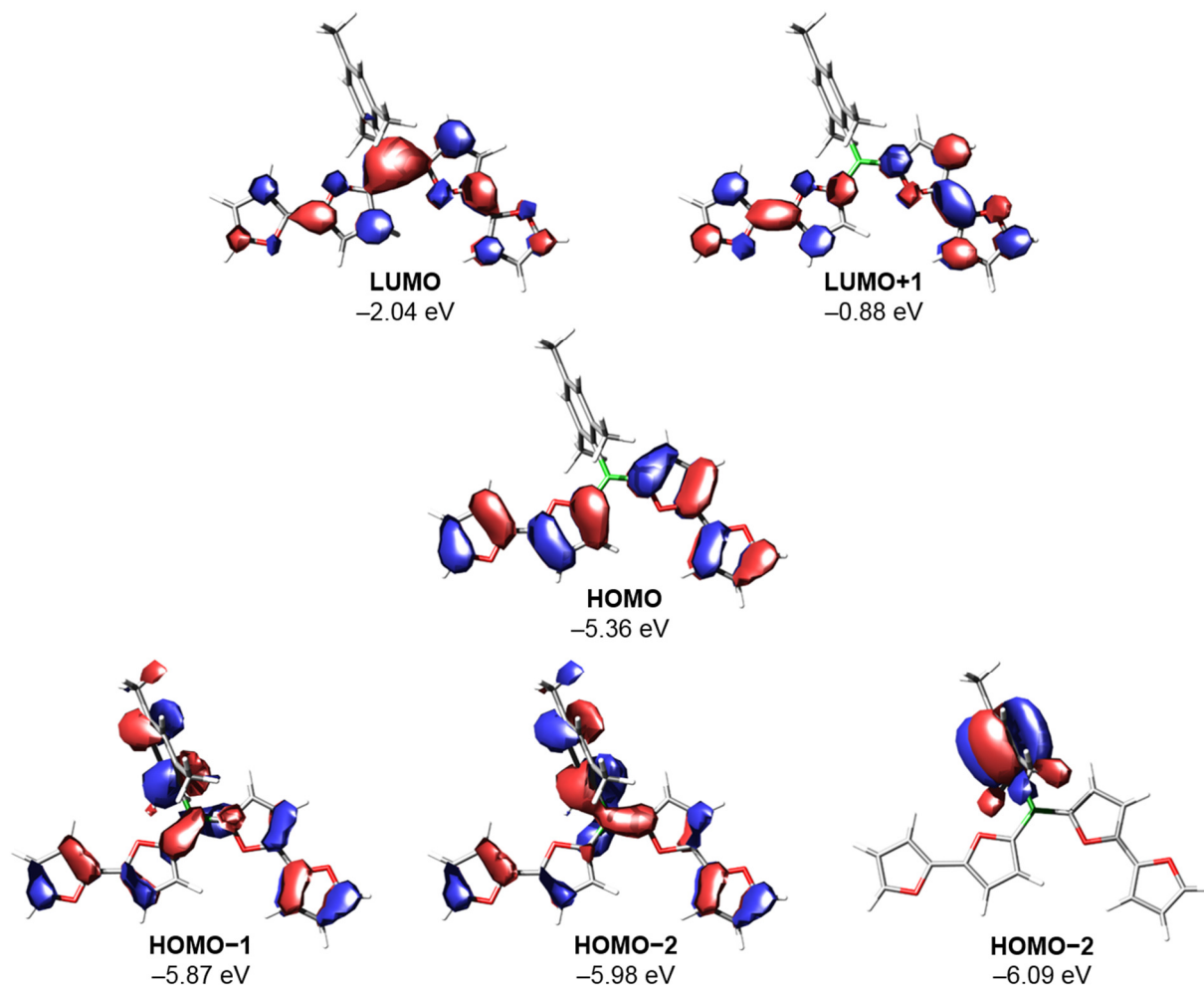


Figure S37. Calculated frontier orbitals of **4'** (isovalue 0.03 a.u.).

Cartesian coordinates [Å] and total energies [a.u.] of optimized stationary points

2a':

Total energy (B3LYP-D3(BJ)/def2-SV(P)): -5978.533161529

O	0.754565	-0.025894	-2.497581
C	1.476939	-0.023971	-1.306010
C	2.823051	-0.027201	-1.640999
C	2.927392	-0.030531	-3.058272
C	1.624982	-0.028099	-3.506248
B	0.691916	-0.015286	0.007844
C	-0.882491	-0.012943	0.025058
C	-1.593117	1.187375	-0.193562
C	-2.992961	1.182969	-0.152132
C	-3.718005	0.010041	0.091499
C	-3.001702	-1.176979	0.289209
C	-1.601435	-1.204990	0.263484
C	-0.846639	2.468902	-0.488833
C	-5.226049	0.028541	0.164484
C	-0.866737	-2.510975	0.472670
C	1.423792	0.010819	1.357117
C	0.944384	0.073916	2.653996
C	2.058225	0.087907	3.540967

C	3.159917	0.031849	2.719752
O	2.813652	-0.013333	1.429724
Br	4.981254	0.010862	3.119679
H	2.063441	0.133283	4.628001
H	-0.112163	0.107494	2.919882
H	-0.073376	2.675488	0.274274
H	-1.527526	3.336260	-0.522900
H	-0.329021	2.407805	-1.464195
H	-0.257476	-2.491041	1.395040
H	-1.566610	-3.360375	0.548618
H	-0.172574	-2.719917	-0.362683
H	-3.549622	-2.109718	0.465218
H	-3.533586	2.121318	-0.320398
H	3.823817	-0.033135	-3.675020
Br	0.937480	-0.025508	-5.239041
H	3.639722	-0.026828	-0.920873
H	-5.651653	0.835404	-0.457431
H	-5.659491	-0.929424	-0.172731
H	-5.574597	0.197029	1.202303

2b':

Total energy (B3LYP-D3(BJ)/def2-SV(P)): -1426.465505390

O	0.750724	-0.016409	-2.493144
C	1.475551	-0.019124	-1.304459
C	2.820733	-0.022240	-1.642628
C	2.920453	-0.020384	-3.060405
C	1.616924	-0.015507	-3.507757
B	0.692149	-0.014328	0.011060
C	-0.882014	-0.012154	0.027979
C	-1.593195	1.186150	-0.200211
C	-2.993107	1.180696	-0.161878
C	-3.717674	0.008800	0.088240
C	-3.000800	-1.176209	0.295512
C	-1.600486	-1.203206	0.272914
C	-0.847393	2.466751	-0.501206
C	-5.225887	0.026594	0.157852
C	-0.865573	-2.507704	0.490545
C	1.425622	0.007167	1.360115
C	0.946781	0.069468	2.657228
C	2.061720	0.078054	3.542873
C	3.165096	0.019685	2.722534
O	2.814222	-0.022027	1.431754
I	5.197584	-0.010972	3.171693
H	2.063958	0.121338	4.630300
H	-0.109453	0.105681	2.924225
H	-0.078185	2.680135	0.264154
H	-1.529631	3.332652	-0.544573
H	-0.325204	2.399507	-1.473639
H	-0.258080	-2.482768	1.413876
H	-1.565308	-3.356939	0.569539
H	-0.169794	-2.720842	-0.342392
H	-3.548299	-2.108363	0.475840
H	-3.534200	2.117450	-0.337567
H	3.817694	-0.021110	-3.676444
I	0.844744	-0.004573	-5.440362
H	3.639680	-0.025163	-0.925053

H	-5.650915	0.826976	-0.472818
H	-5.657753	-0.935038	-0.170854
H	-5.576736	0.204973	1.193255

5:

Total energy (B3LYP-D3(BJ)/def2-SV(P)): -1561.207217474

C	0.252447	-0.387049	2.568198
C	1.371948	-0.568249	3.353528
C	2.491461	-0.491229	2.475561
C	1.990179	-0.268108	1.208953
O	0.626217	-0.205103	1.269342
H	1.376648	-0.735143	4.428618
H	3.543705	-0.588183	2.739093
C	2.594876	-0.100525	-0.087517
S	4.329195	-0.163997	-0.293125
C	4.187051	0.106231	-1.998045
C	2.875979	0.237759	-2.386492
C	1.963160	0.120489	-1.298856
H	0.878147	0.193656	-1.388165
H	2.571679	0.413457	-3.421032
H	5.084342	0.152253	-2.615717
C	-1.150085	-0.357966	2.857176
C	-2.269255	-0.170495	2.072844
C	-3.388999	-0.251899	2.950120
C	-2.888198	-0.484059	4.215293
O	-1.524274	-0.547794	4.154787
H	-2.273571	0.003647	0.998903
H	-4.441113	-0.152517	2.686971
C	-3.493497	-0.662952	5.509969
S	-5.227861	-0.600390	5.715483
C	-5.086671	-0.888729	7.417510
C	-3.775877	-1.025495	7.805089
C	-2.862484	-0.897292	6.719169
H	-1.777586	-0.972572	6.808111
H	-3.472183	-1.212696	8.837788
H	-5.984260	-0.940463	8.034298

6:

Total energy (B3LYP-D3(BJ)/def2-SV(P)): -915.4046364487

C	0.274378	-0.362287	2.483932
C	1.420791	-0.532174	3.232064
C	2.512648	-0.447732	2.319319
C	1.962673	-0.231292	1.073862
O	0.603240	-0.178619	1.172043
H	1.460227	-0.697366	4.306786
H	3.574764	-0.534274	2.539179
C	2.532241	-0.062463	-0.233184
C	1.981763	0.156345	-1.476360
C	3.082600	0.235351	-2.389339
O	3.890367	-0.121356	-0.332455
C	4.213386	0.059589	-1.639751
H	5.275666	0.036745	-1.873011
H	3.036270	0.401577	-3.464965
H	0.920440	0.247501	-1.698066
C	-1.118806	-0.348657	2.817443
C	-2.265293	-0.179846	2.069165

C	-3.357625	-0.274867	2.980311
C	-2.807771	-0.494987	4.225182
O	-1.447983	-0.539573	4.128204
H	-2.304518	-0.009310	0.995257
H	-4.420004	-0.193603	2.759655
C	-3.377912	-0.676661	5.530254
C	-2.827338	-0.894499	6.773549
C	-3.929103	-0.994219	7.683368
O	-4.736985	-0.637858	5.626466
C	-5.060516	-0.830932	6.931909
H	-6.123600	-0.825272	7.162560
H	-3.882964	-1.165628	8.758184
H	-1.765371	-0.971934	6.997332

3':

Total energy (B3LYP-D3(BJ)/def2-SV(P)): -1935.189219178

C	0.346012	-1.137169	7.912612
C	-1.019654	-1.123680	7.689509
S	-1.895228	-1.384527	9.178766
C	-0.424222	-1.507734	10.079941
C	0.682445	-1.356942	9.278626
C	-1.712788	-0.928816	6.439831
C	-3.057357	-0.879936	6.107570
C	-3.105202	-0.655127	4.708944
C	-1.800968	-0.576525	4.243255
O	-0.961737	-0.749864	5.331936
B	-1.255949	-0.362565	2.826657
C	-2.287316	-0.132462	1.656013
C	-2.878380	1.134923	1.455118
C	-3.789055	1.319140	0.407042
C	-4.141803	0.272383	-0.454190
C	-3.543777	-0.976724	-0.249408
C	-2.622880	-1.191298	0.784518
C	-2.518609	2.295819	2.356196
C	-5.156281	0.481459	-1.553014
C	-1.978486	-2.548797	0.954495
C	0.246955	-0.388227	2.542245
O	0.661441	-0.202050	1.232482
C	2.005021	-0.268141	1.182026
C	2.511930	-0.496179	2.453401
C	1.388789	-0.572217	3.312158
C	2.621810	-0.099505	-0.110301
S	4.354681	-0.173513	-0.314884
C	4.213025	0.107742	-2.015786
C	2.902120	0.250498	-2.405270
C	1.989253	0.132710	-1.319121
H	3.564145	-0.594801	2.717127
H	1.387981	-0.744782	4.386737
H	-2.854811	2.121793	3.394840
H	-1.423904	2.447287	2.398647
H	-2.976182	3.236524	2.005331
H	-6.190189	0.376975	-1.169620
H	-5.032273	-0.256716	-2.364470
H	-5.074712	1.491415	-1.992874
H	-4.233872	2.309531	0.255873
H	-3.798545	-1.807925	-0.916905

H	-0.895791	-2.501848	0.734701
H	-2.079961	-2.920176	1.990967
H	-2.427728	-3.298274	0.280755
H	-3.991299	-0.558509	4.082208
H	-3.893102	-0.992902	6.796774
H	0.903935	0.212874	-1.402343
H	2.600056	0.434690	-3.438879
H	5.110117	0.151990	-2.634100
H	1.072732	-0.990878	7.111748
H	1.706992	-1.401617	9.655134
H	-0.460654	-1.685490	11.155155

4':

Total energy (B3LYP-D3(BJ)/def2-SV(P)): -1289.386741232

O	3.916438	-0.112992	-0.348410
C	2.557358	-0.061474	-0.252090
C	2.007398	0.159538	-1.494990
C	3.108294	0.248259	-2.404909
C	4.239201	0.075374	-1.652458
C	1.975061	-0.234522	1.049511
O	0.634541	-0.183869	1.135732
C	0.265420	-0.371639	2.459946
C	1.433852	-0.539909	3.193093
C	2.530163	-0.453257	2.300426
B	-1.226856	-0.359144	2.795663
C	-2.302265	-0.136843	1.663761
C	-2.894076	1.131390	1.471836
C	-3.846517	1.308302	0.460292
C	-4.240216	0.253277	-0.372662
C	-3.640882	-0.996749	-0.177484
C	-2.679256	-1.204095	0.820219
C	-2.490124	2.300281	2.343105
C	-5.298432	0.454920	-1.430898
C	-2.035894	-2.563046	0.981997
C	-1.720146	-0.575729	4.230747
C	-3.006415	-0.653263	4.744551
C	-2.910484	-0.877311	6.141608
C	-1.555041	-0.925715	6.417957
O	-0.840373	-0.748622	5.288495
C	-0.828783	-1.121142	7.642354
O	-1.559500	-1.302744	8.779033
C	-0.686970	-1.464391	9.804881
C	0.602509	-1.391197	9.351112
C	0.514944	-1.167263	7.940264
H	3.592341	-0.537557	2.521691
H	1.467609	-0.708302	4.267871
H	-2.770831	2.134137	3.399398
H	-1.394942	2.453647	2.326447
H	-2.967335	3.237407	2.009211
H	-6.316014	0.359658	-1.003863
H	-5.211385	-0.292880	-2.238357
H	-5.230816	1.459488	-1.885225
H	-4.292042	2.299344	0.315634
H	-3.927735	-1.834582	-0.823357
H	-0.959354	-2.522235	0.732430
H	-2.110330	-2.926284	2.023710

H	-2.506553	-3.315603	0.326520
H	-3.914073	-0.555729	4.149497
H	-3.713560	-0.991167	6.866926
H	0.944625	0.245860	-1.713199
H	3.063827	0.418887	-3.479884
H	5.301890	0.060065	-1.885207
H	1.331737	-1.053350	7.230162
H	1.507931	-1.485363	9.949348
H	-1.131212	-1.620052	10.785739

References

- [1] a) A. Lik, L. Fritze, L. Müller and H. Helten, *J. Am. Chem. Soc.* 2017, **139**, 5692. b) Y. Dienes, S. Durben, T. Karpati, T. Neumann, U. Englert, L. Nyulaszi and T. Baumgartner, *Chem. Eur. J.* 2007, **13**, 7487. c) D. C. Ebner, J. T. Bagdanoff, E. M. Ferreira, R. M. McFadden, D. D. Caspi, R. M. Trend and B. M. Stoltz, *Chem. Eur. J.* 2009, **15**, 12978.
- [2] SADABS: Area-Detector Absorption Correction; Siemens Industrial Automation, Inc.: Madison, WI, 1996.
- [3] O. V. Dolomanov, L. J. Bourhis, R. J. Gildea, J. A. K. Howard, and H. J. Puschmann, *J. Appl. Cryst.* 2009, **42**, 339.
- [4] a) G. M. Sheldrick, *Acta Crystallogr., Sect. A* 2008, **64**, 112; b) G. M. Sheldrick, *Acta Crystallogr., Sect. C* 2015, **71**, 3.
- [5] Turbomole: R. Ahlrichs, M. Bär, M. Häser, H. Horn and C. Kölmel, *Chem. Phys. Lett.* 1989, **162**, 165–169.
- [6] a) P. A. M. Dirac, *Proc. R. Soc. London, Ser. A* 1929, **123**, 714–733; b) J. C. Slater, *Phys. Rev.* 1951, **81**, 385–390; c) A. D. Becke, *Phys. Rev. A* 1988, **38**, 3098–3100; d) C. Lee, W. Yang, R. G. Parr, *Phys. Rev. B* 1988, **37**, 785–789; e) A. D. Becke, *J. Chem. Phys.* 1993, **98**, 5648–5652.
- [7] A. Schäfer, H. Horn and R. Ahlrichs, *J. Chem. Phys.* 1992, **97**, 2571–2577.
- [8] a) S. Grimme, J. Antony, S. Ehrlich and H. Krieg, *J. Chem. Phys.* 2010, **132**, 154104; b) S. Grimme, S. Ehrlich and L. Goerigk, *J. Comput. Chem.* 2011, **32**, 1456–1465.
- [9] P. Deglmann, F. Furche and R. Ahlrichs, *Chem. Phys. Lett.* 2002, **362**, 511–518; b) P. Deglmann and F. Furche, *J. Chem. Phys.* 2002, **117**, 9535–9538.
- [10] a) R. Bauernschmitt and R. Ahlrichs, *Chem. Phys. Lett.* 1996, **256**, 454–464; b) R. Bauernschmitt and R. Ahlrichs, *J. Chem. Phys.* 1996, **104**, 9047–9052; c) F. Furche and D. Rappoport, in *Density functional methods for excited states: equilibrium structure and electronic spectra*, ed. M. Olivucci, Elsevier, Amsterdam, 2005.